2016 Spring

# “Advanced Physical Metallurgy”

# - Bulk Metallic Glasses -

04.18.2016

Eun Soo Park

Office: 33-313
Telephone: 880-7221
Email: espark@snu.ac.kr
Office hours: by appointment

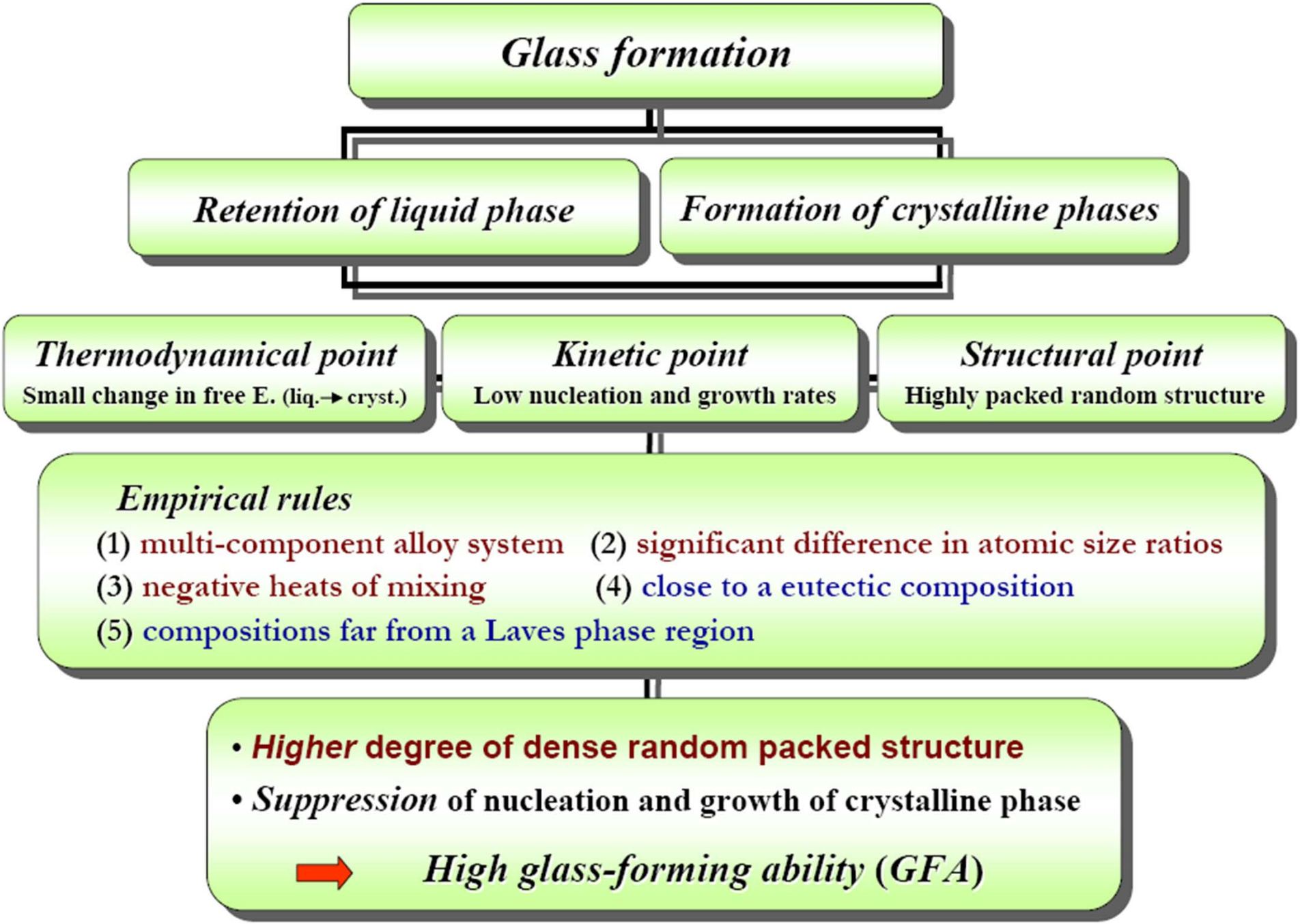
Glass formation
Retention of liquid phase
Formation of crystalline phases
Thermodynamical point
Small change in free E. (liq.→cryst.)
Kinetic point
Low nucleation and growth rates
Structural point
Highly packed random structure
Empirical rules
(1) multi-component alloy system
(2) significant difference in atomic size ratios
(3) negative heats of mixing
(4) close to a eutectic composition
(5) compositions far from a Laves phase region
• Higher degree of dense random packed structure
• Suppression of nucleation and growth of crystalline phase
High glass-forming ability (GFA)

# Representative GFA Parameters

## Based on thermal analysis ($T_g$, $T_x$ and $T_l$): thermodynamic and kinetic aspects

$T_{rg} = T_g/T_l$ — D. Turnbull et al., *Contemp. Phys.*, 10, 473 (1969)

$K = (T_x - T_g) / (T_l - T_x)$ — A. Hruby et al., *Czech.J.Phys.*, B22, 1187 (1972)

$\Delta T^* = (T_m^{mix} - T_l) / T_m^{mix}$ — I. W. Donald et al., *J. Non-Cryst. Solids*, 30, 77 (1978)

$\Delta T_x = T_x - T_g$ — A. Inoue et al., *J. Non-Cryst. Solids*, 156-158, 473 (1993)

$\gamma = T_x / (T_l + T_g)$ — Z.P. Lu and C. T. Liu, *Acta Materialia*, 50, 3501 (2002)

## Based on thermodynamic and atomic configuration aspects

$\sigma = \Delta T^* \times P'$ — E. S. Park et al., *Appl. Phys. Lett.*, 86, 061907 (2005)

*ΔT* :* Relative decrease of melting temperature + *P'* : atomic size mismatch

: can be calculated simply using data on melting temp. and atomic size

# *GFA Parameters on the basis of thermodynamic or kinetic aspects :*

## 1) $\Delta T_x$ parameter = $T_x - T_g$

- quantitative measure of glass stability toward crystallization upon reheating the glass above $T_g$: stability of glass state
- cannot be considered as a direct measure for GFA

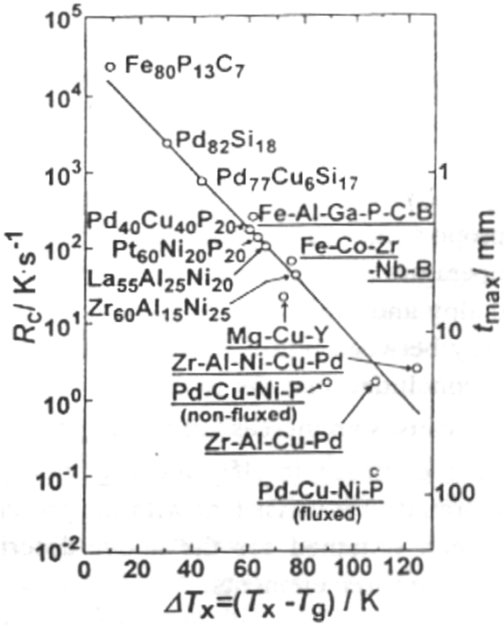


## 2) K parameter = $(T_x-T_g)/(T_l-T_x) = \Delta T_x/(T_l-T_x)$

- based on thermal stability of glass on subsequent reheating
- includes the effect of $T_l$ , but similar tendency to $\Delta T_x$

## 3) $\Delta T^*$ parameter = $(T_m^{mix} - T_l)/ T_m^{mix}$

- $$T_m^{mix} = \sum_i^n n_i \cdot T_m^i$$

( where $n_i$ and $T_m^i$ are the mole fraction and melting point, respectively, of the $i$ th component of an $n$-component alloy.)

- evaluation of the stability of the liquid at equilibrium state
- alloy system with deep eutectic condition ~ good GFA
- for multi-component BMG systems: insufficient correlation with GFA

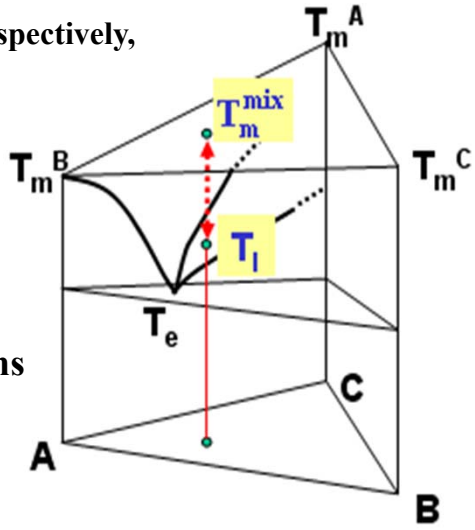


➡ $T_m^{mix}$ represents the fractional departure of $T_m$ with variation of compositions and systems from the simple rule of mixtures melting temperature

## *GFA Parameters on the basis of thermodynamic or kinetic aspects :*

### 4) $T_{rg}$ parameter = $T_g/T_l$

- kinetic approach to avoid crystallization before glass formation
- Viscosity at $T_g$ being constant, the higher the ratio $T_g/T_l$, the higher will be the viscosity at the nose of the CCT curves, and hence the smaller $R_c$
- $T_l$ ↓and $T_g$ ↑ ► lower nucleation and growth rate ► GFA ↑

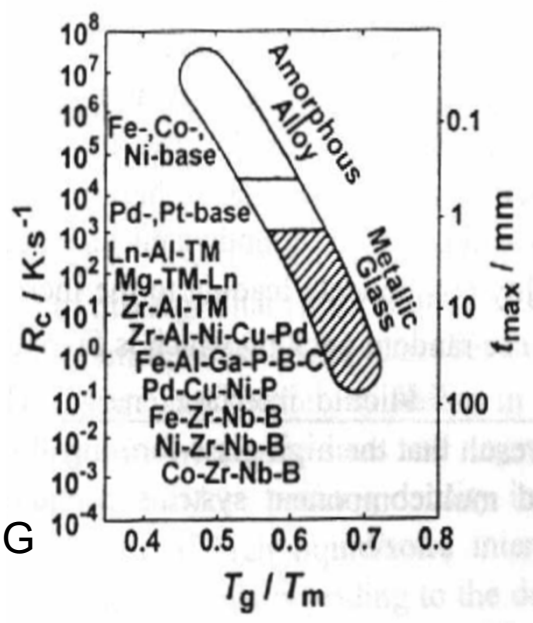


- ▪ significant difference between $T_l$ and $T_g$ in multi-component BMG
- ▪ insufficient information on temperature-viscosity relationship

► insufficient correlation with GFA

### 5) γ parameter = $T_x$ / ($T_l$ + $T_g$)

- thermodynamic and kinetic view points - relatively reliable parameter
- stability of equilibrium and metastable liquids: $T_l$ and $T_g$
- resistance to crystallization: $T_x$

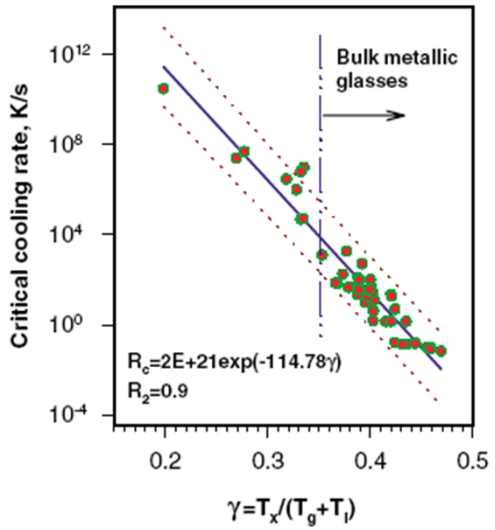

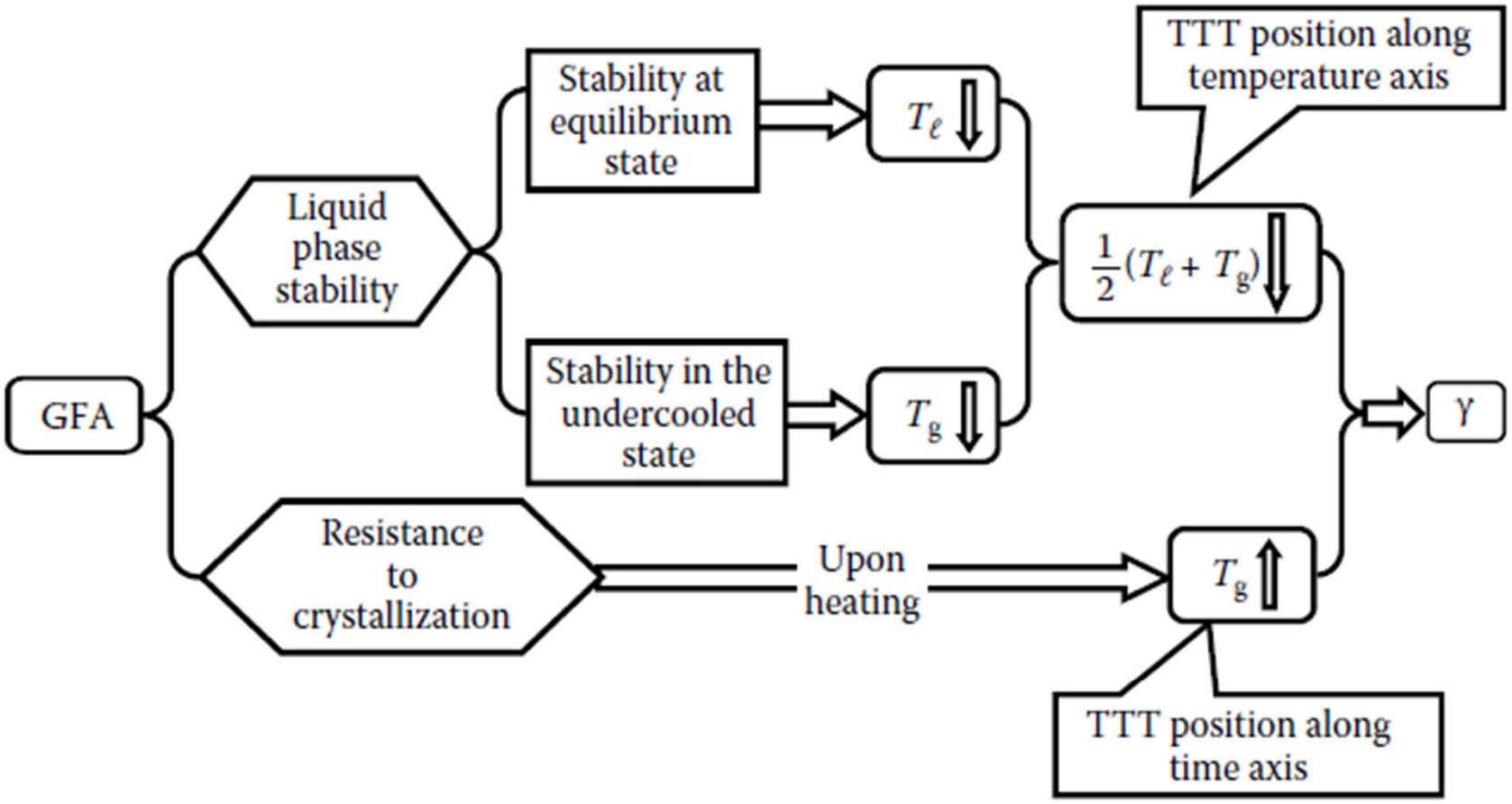


**FIGURE 3.8**
Schematic to illustrate the different factors involved in deriving the γ parameter to explain the GFA of alloys. (Reprinted from Lu, Z.P. and Liu, C.T., *Intermetallics*, 12, 1035, 2004. With permission.)

# GFA Parameters *on the basis of thermodynamic or kinetic aspects*

| GFA parameters | Expression | Year established | |
|---|---|---|---|
| $T_{rg}$ | $T_g / T_l$ | 1969 | D.Turnbull,Contemp.Phys.10(1969) 473 |
| K | $(T_x-T_g) / (T_l-T_x)$ | 1972 | A.Hruby, Czech. J.Phys. B 22 (1972) 1187 |
| $\Delta T^*$ | $(T_m^{mix}-T_l) / T_m^{mix}$ | 1978 | I.W.Donald, J.Non-Cryst.Solids 30 (1978) 77 |
| $\Delta T_x$ | $T_x - T_g$ | 1993 | A.Inoue, J.Non-Cryst.Solids 156-158(1993)473 |
| $\gamma$ | $T_x / (T_l+T_g)$ | 2002 | Z.P.Lu, C.T.Liu, Acta Mater. 50 (2002) 3501 |
| $\delta$ | $T_x / (T_l-T_g)$ | 2005 | Q.J.Chen,Chiness Phys.Lett.22 (2005) 1736 |
| $\alpha$ | $T_x / T_l$ | 2005 | K.Mondal, J.Non-Cryst.Solids 351(2005) 1366 |
| $\beta$ | $T_x / T_g + T_g / T_l$ | 2005 | K.Mondal, J.Non-Cryst.Solids 351(2005) 1366 |
| $\varphi$ | $(T_g / T_l)(T_x-T_g / T_g)^a$ | 2007 | G.J.Fan,J.Non-Cryst. Solids 353 (2007) 102 |
| $\gamma_m$ | $(2T_x - T_g) / T_l$ | 2007 | X.H.Du,J.Appl.phys.101 (2007) 086108 |
| $\beta$ | $(T_g / T_l - T_g)(T_g / T_l - T_g)$ | 2008 | Z.Z.Yuan, J. Alloys Compd.459 (2008) |
| $\xi$ | $\Delta T_x / T_x + T_g / T_l$ | 2008 | X.H.Du,Chinese Phys.B 17(2008) 249 |

*No universal model* to predict and evaluate what families of alloy compositions are likely to form BMGs

**Combination of categories**

that are viewed as decisive in the formation of amorphous alloys

***New criterion***

for predicting and evaluating Glass Forming Ability

- useful guideline for BMG alloy system design

- save time and experimental cost

→ new alloy system with enhanced GFA

# σ parameter (thermodynamic and atomic configuration aspects)

$\Delta T^*$ : Relative decrease of melting temp.

➡ liquid phase stability

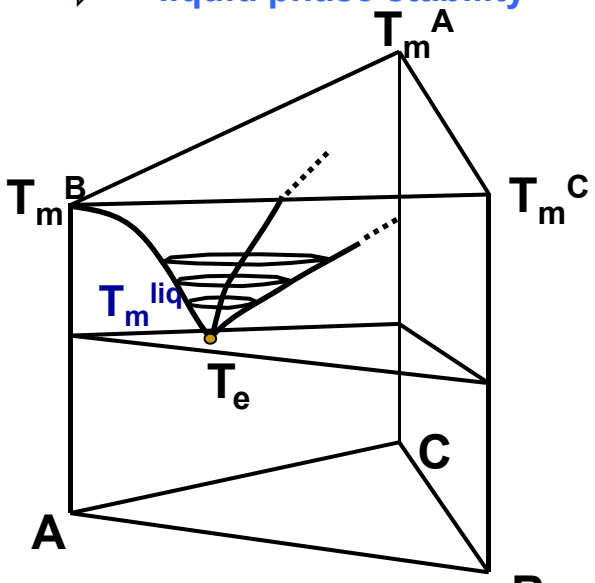


Deep eutectic condition

×

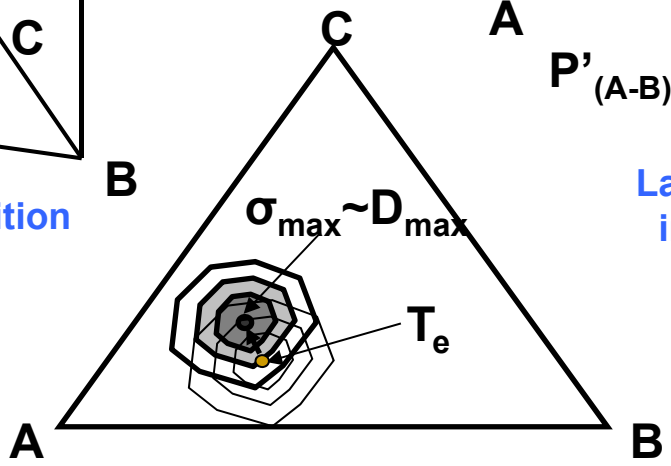


$P'$ : Effective atomic mismatch per solute atom

➡ solid phase stability

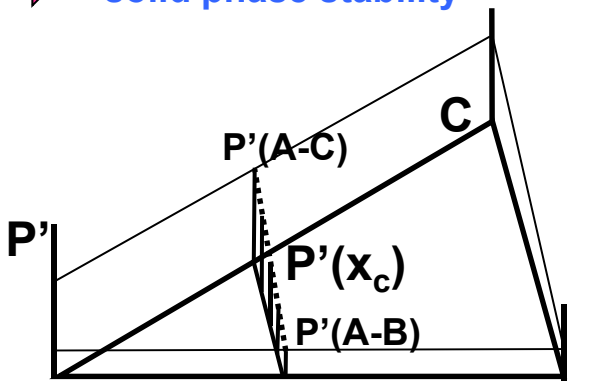


$P'_{(A-B)} \leq P'(Xc) \leq P'_{(A-C)}$

Large difference in atomic size

**New criterion for GFA, σ parameter** $\sigma = \Delta T^* \times P'$

* Appl. Phys. Lett., 86, 061907 (2005)

## *Motivation for new criterion* (2) : Role of characteristic temp. for GFA

| Positive Temperature Factor | | Negative Temperature Factor |
|---|---|---|
| $T_x$ | $\Delta T_x$ | $T_g$ |
| $T_g$ | $T_{rg}$ | $T_l$ |
| $T_m^{mix} - T_l$ | $\Delta T^*$ | $T_m^{mix}$ |
| $\Delta T_x$ | $K$ | $T_l - T_x$ |
| $T_x$ | $\gamma$ | $T_l + T_g$ |

**With $T_x$ ↑and $T_l$ ↓, GFA parameter ↑. But, the role of $T_g$ is not consistent.**

## *Points of issue for new GFA parameter*

**1. Combination of categories for glass formation**

- γ parameter: thermodynamic/ kinetic aspects

➡ New parameter combining thermodynamic/ kinetic aspects

**2. Temperature scale for GFA parameter**

$\Delta T_x$ parameter : $T_x - T_g$

K parameter : $T_g - T_x - T_l$

$T_{rg}$ parameter : $T_g - T_l$

γ parameter : $T_g - T_x - T_l$

$\Delta T^*$ parameter : $T_l - T_m^{mix}$

➡ New parameter covering temperature range $T_g - T_x - T_l - T_m^{mix}$ with considering about two different role of $T_g$

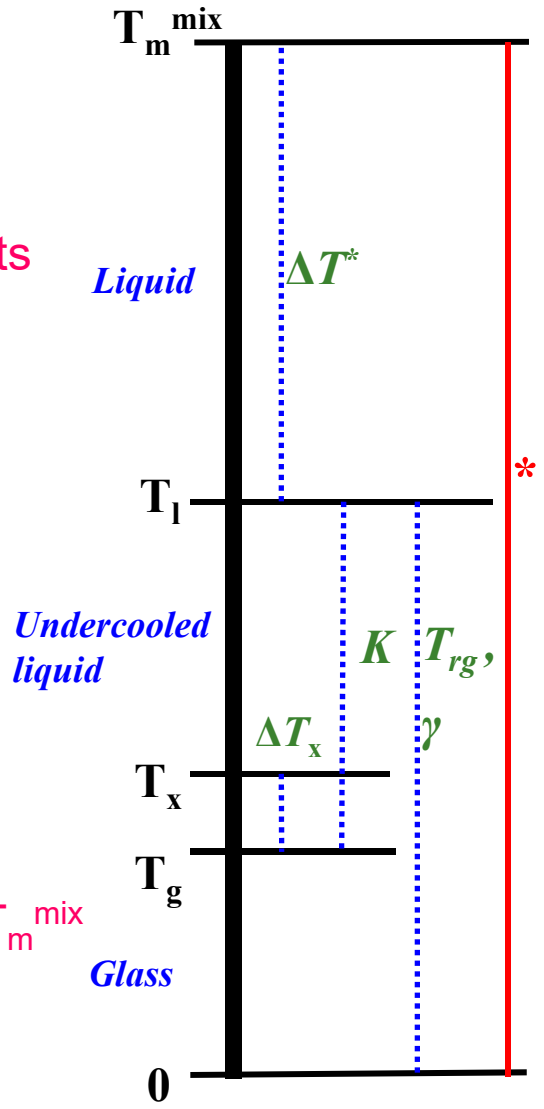

## *A new criterion for GFA* : ε parameter

### a. Liquid phase stability :

- Relative stability of stable liquid : distance from the $T_m^{mix}$ to liquidus melting temp.,

$$\Delta T_m = T_m^{mix} - T_l \qquad (\gamma \text{ parameter: } T_l)$$

- Stability of metastable liquid : range of supercooled liquid,

$$\Delta T_x = T_x - T_g \qquad (\gamma \text{ parameter: } T_g)$$

### b. Resistance to crystallization : $T_x$ ($\gamma$ parameter: $T_x$)

- relative difficulties for the formation (nucleation and crystal growth)

  of the competing crystalline phases in various BMG forming alloy system

- Retarding incubation time for crystallization : relative position of the CCT curves along the time axis

### c. nomalizing : $T_m^{mix}$

- Exclusion of systematic and compositional effects in various BMG alloy systems

## A New criterion for GFA of BMGs

$$\varepsilon = \frac{\Delta T_m + \Delta T_x + T_x}{T_m^{mix}}$$

E. S. Park et al., *JAP (2015)*

# ε parameter (thermodynamic and kinetic aspects)

## A New criterion for GFA of BMGs

$$\varepsilon = \frac{\Delta T_m + \Delta T_x + T_x}{T_m^{mix}}$$

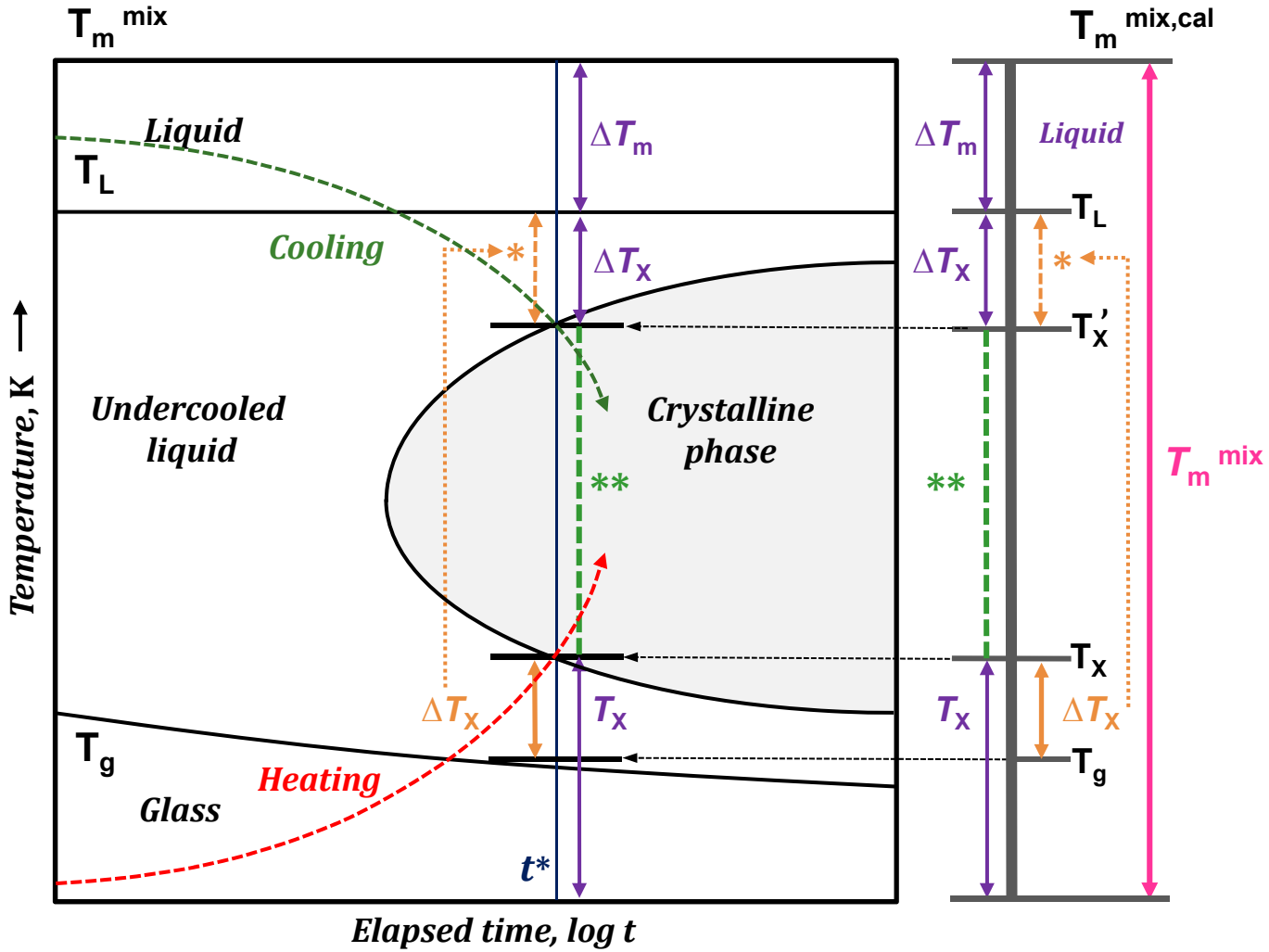

# Improvement of GFA

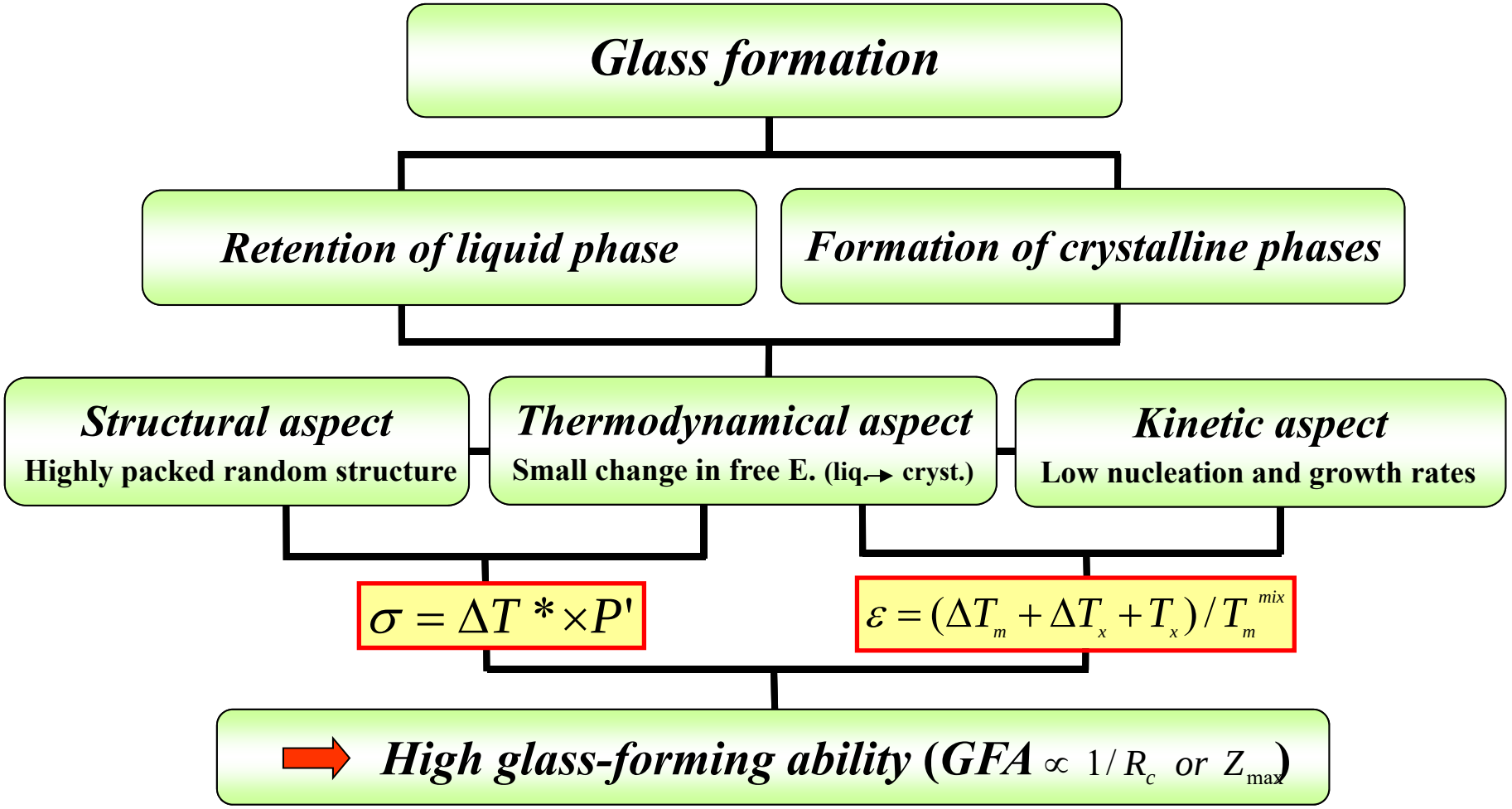


**In estimating the GFA, the combinational effects of thermodynamic, kinetic and structural aspects for glass formation should be considered.**

$$\mathrm{GFA} \propto (\varepsilon,\ V_{epsilon} = \frac{V(T_m^{mix} - T_l) + V(T_x - T_g) + V(T_x)}{V(T_m^{mix})})$$

$$\kappa = (1-\varepsilon)\times(1-V_\varepsilon)$$

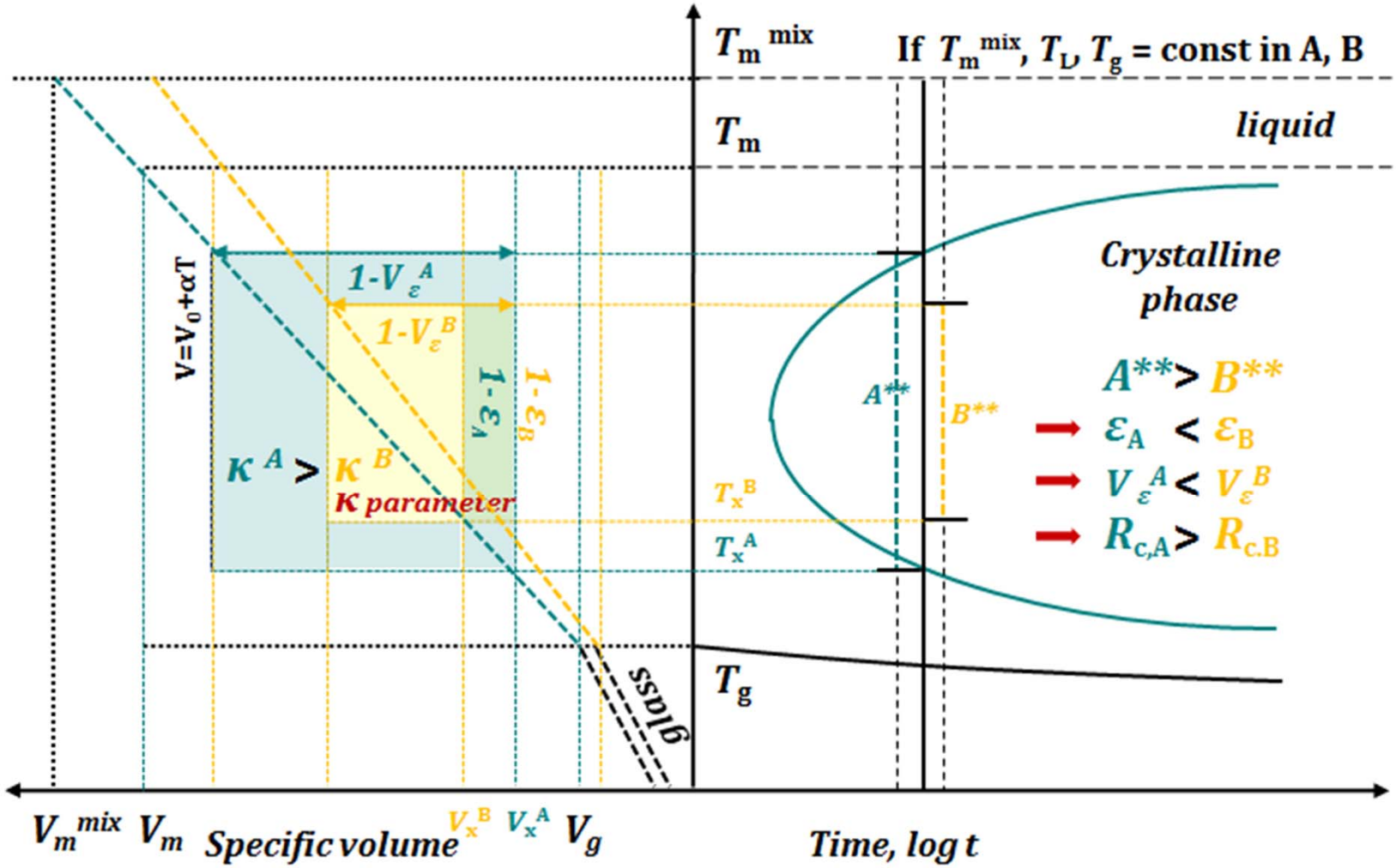

# 4 Synthesis of Bulk Metallic Glasses

Metallic glasses: produced by rapidly solidifying metallic melts to cooling rate about $10^6$K/s

⇕

BMG : Produced by relatively slow solidification rates of about $10^3$ K/s or less

## 4.2 Principles of Rapid Solidification Processing: Huge departure from equilibrium

1) A small quantity of the molten metal is ejected using a shock wave on to a conducting substrate. The molten metal spreads in the form of a thin layer, typically a few tens of micrometers (but usually about 20-50 μm) in thickness, and the heat is extracted rapidly by conducting copper substrate.

2) Basic requirements to achieve high solidification rates:
   a. Forming a thin layer (film or ribbon) of the molten metal
   b. Intimate thermal contact with a good heat-conducting substrate to rapidly extract the heat from the liquid metal

3)

$$R = \frac{A}{x^2}$$

where
$x$ is the distance from the splat/substrate interface
the constant $A$ is a function of the material properties and initial temperatures, but is independent of $x$

The value of $A$ is $8.1 \times 10^{-3}$ m$^2$ K s$^{-1}$ for ideal cooling (when the heat transfer coefficient is ∞) and it is less for nonideal cooling conditions. For example, assuming an average value of $A = 10^{-3}$ m$^2$ K s$^{-1}$, for rough estimates, the solidification rate achieved will be approximately $10^5$ K s$^{-1}$ for $x = 100\,\mu$m and $10^9$ K s$^{-1}$ for $x = 1\,\mu$m. The typical thickness of a rapidly solidified foil is about 50 μm, and therefore the foil would have solidified at a rate of approximately $10^6$ K s$^{-1}$. These examples serve to illustrate that it is necessary to have as small a section thickness as possible to achieve high solidification rates.

## 4.3 General Techniques to Achieve High Rates of Solidification

"Energize and quench" – increase the free energy of the system (by either raising the temperature, or pressure or the input of mechanical energy, or by other means) and subsequently quenching the material to either retain the metastable phase or to use it as an intermediate step to achieve the desired microstructure and/or properties → Some very interesting properties

4.4 Melt Spinning: the most commonly used method to produce long and continuous rapidly solidified ribbons, wires, and filaments

- Free flight melt-spinning, Chill block melt-spinning

: a small quantity of the alloy is melted inside a crucible or by levitation methods, and then ejected by pressurization trough a fine nozzle onto a fast-rotating copper wheel.

- Crucible material: based on it chemical compatibility with with the melts, its temperature handling capability, its resistance to thermal shock, its low thermal conductivity, and its low porosity ex) dense alumina and quartz
- Nozzle: about 50 μm to 1250 μm, alumina, graphite, SiC, Sapphire, and pyrex glass
- Ejection pressures: 5-70 kPa depending on desired melt delivery rate, high ejection pressures → improvement of the wetting pattern and better thermal contact between the melt puddle and the substrate.

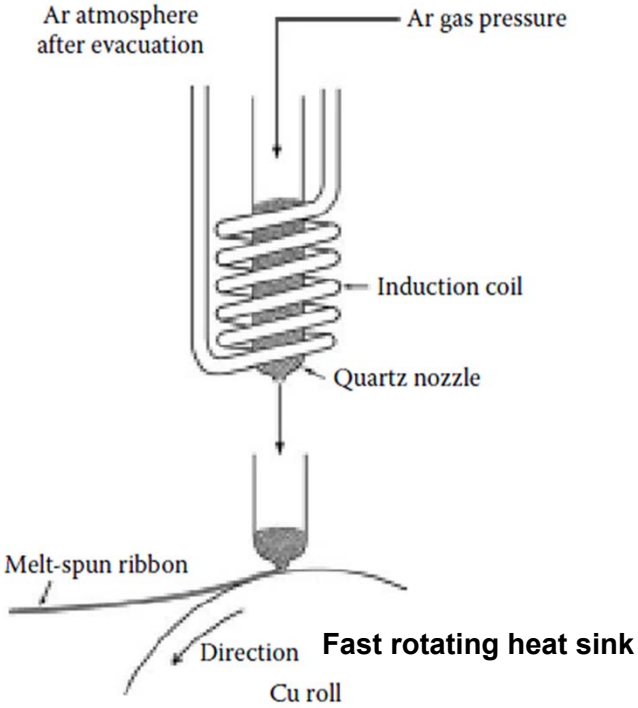


FIGURE 4.1
Schematic illustration of the melt-spinning process.

## 4.4 Melt Spinning: the most commonly used method to produce long and continuous rapidly solidified ribbons, wires, and filaments

- Wheel for melt-spinning:

  a) extract the heat from the ribbon as quickly as possible

  b) a variety of materials including <u>copper</u>, stainless steel, chromium, and molybdenum

  c) outer surface of the wheel is generally polished to remove any surface roughness

  due to wheel side of the cast ribbon → almost an exact replica of the wheel surface

  d) Wheel speed is an important parameter in determining the thickness of the ribbon

  ex_$Fe_{40}Ni_{40}B_{20}$ alloy, 250 mm diameter copper wheel,

  substrate velocity o 26.6 m/s → 37 μm, substrate velocity o 46.5 m/s → 22 μm,

- Operation: carried out in vacuum, air, or inert atmosphere, or reactive gas depending on the chemical and physical properties of the charge

- Solidification rate: typically about $10^5$-$10^6$ K/s,

- Typical dimensions of ribbons: 2-5 mm→ <u>can be increased using the planar flow casting method</u>

- Thickness: 20-50 μm → <u>cannot be increased</u>

⇨ These thin ribbon used to measure the thermal properties ($T_g$, $T_x$, and $T_l$) using the DSC and or DTA methods. This is appropriate because the thermal properties of the glass do not depend on the dimensions of the glass specimen (in general). → **Calculation of GFA parameters**

- **Melt-spinning method**

Thin film

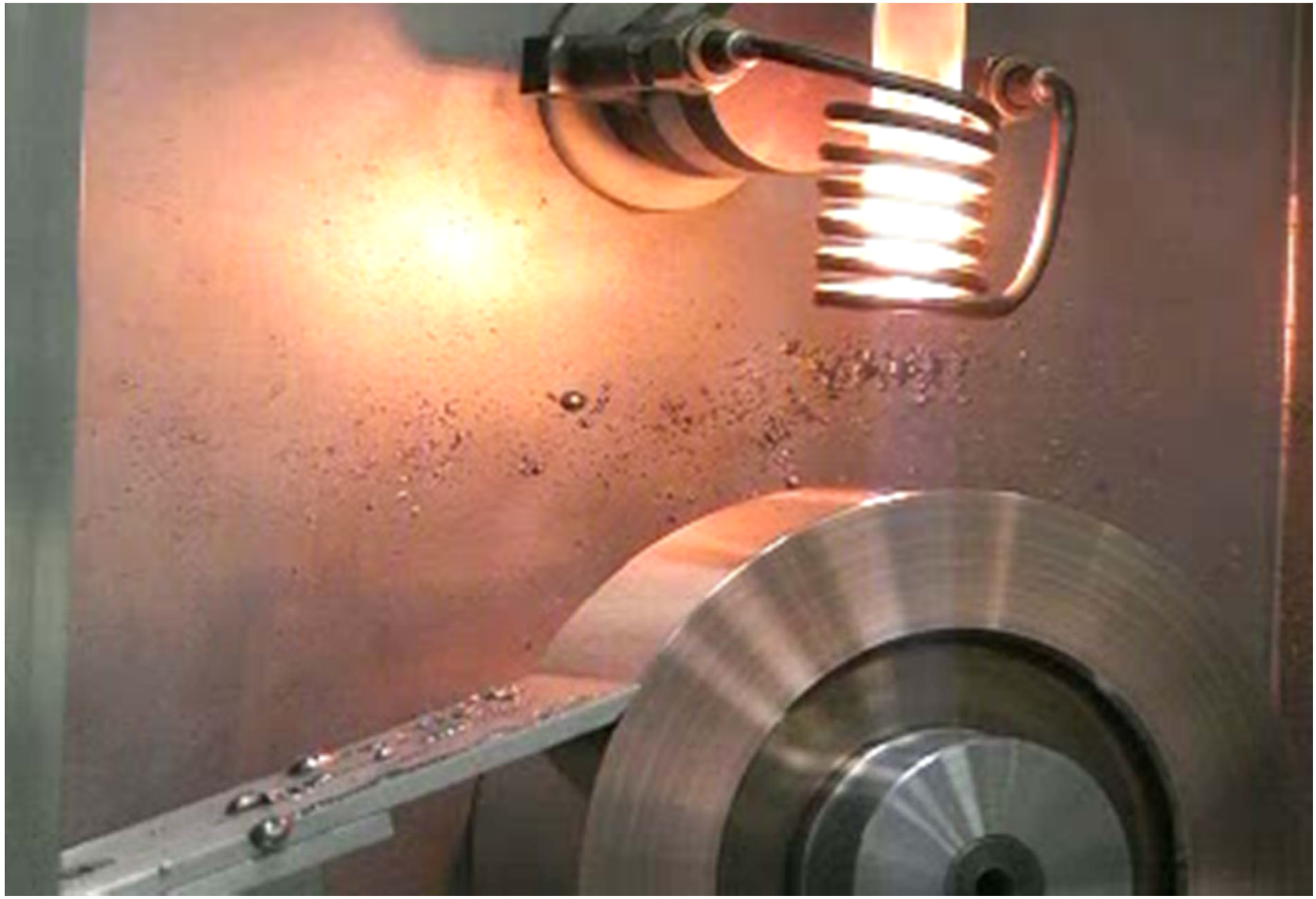

# 4.5 Bulk Metallic Glass

## * History of Metallic Glasses

- First amorphous metal produced by evaporation in 1934.

  ** j. Kramer, Annalen der Phys. 1934; 19: 37.*

- First amorphous alloy(CoP or NiP alloy)

  produced by electro-deposition in 1950.

  ** A. Brenner, D.E. Couch, E.K. Williams, J. Res. Nat. Bur. Stand. 1950: 44; 109.*

- First metallic glass ($Au_{80}Si_{20}$)

  produced by splat quenching at Caltech by Pol Duwez in 1957.

  ** W. Klement, R.H. Willens, P. Duwez, Nature 1960; 187: 869.*

- First bulk metallic glass ($Pd_{77.5}Cu_6Si_{16.5}$)
  produced by droplet quenching at Harvard Univ.
  by H.S. Chen and D. Turnbull in 1969

  ** H.S. Chen and D. Turnbull, Acta Metall. 1969; 17: 1021.*

  produced by water quenching of PdTMSi, Pt-Ni-P and Pd-Ni-P system
  by H.S. Chen in 1974 ( long glassy roads, 1-3 mm in diameter and several centimeters in length)

  ** H.S. Chen, Acta Metall. 1974; 22: 1505*

- First bulk metallic glass: $Pd_{77.5}Cu_6Si_{16.5}$ ($T_{rg}$=0.64)

By droplet quenching (CR~800 K/s)

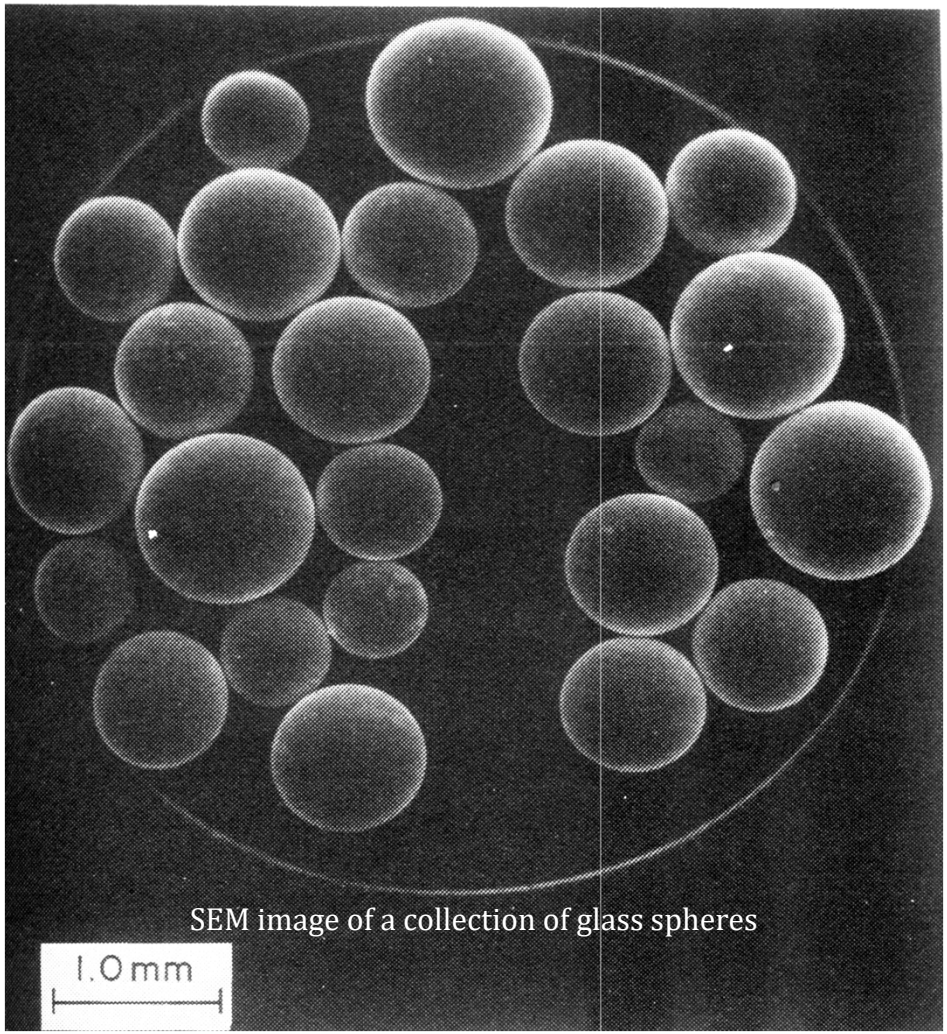


SEM image of a collection of glass spheres

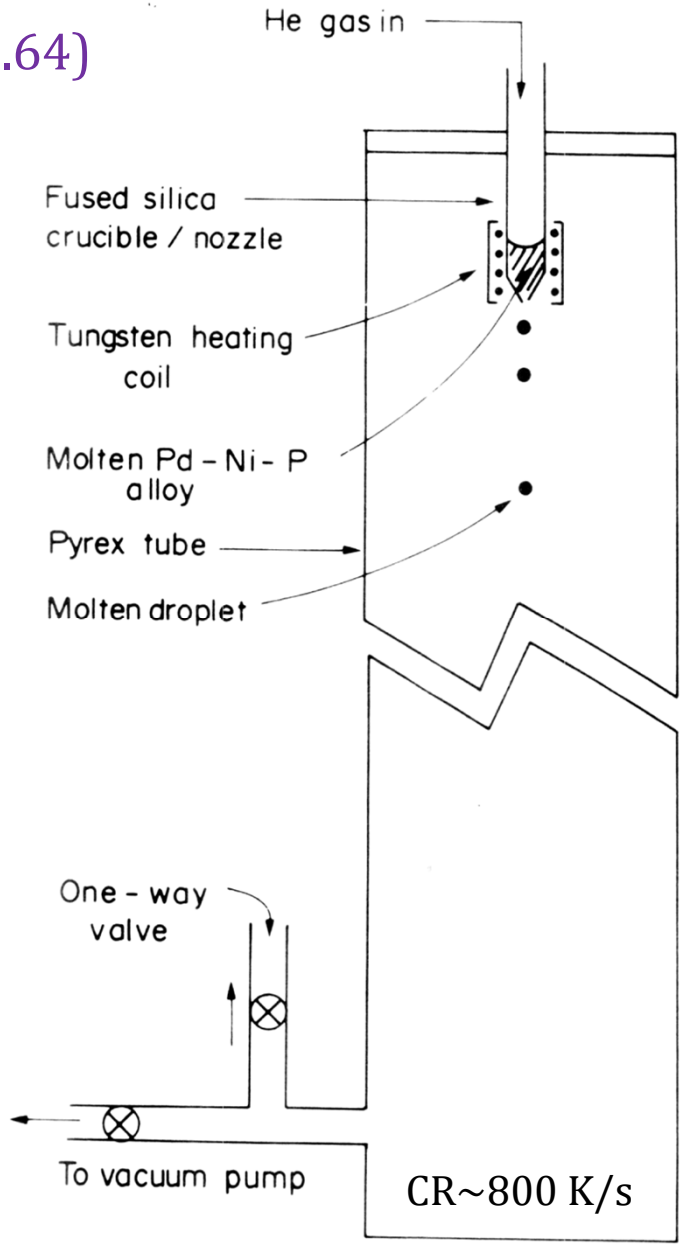


** H.S. Chen and D. Turnbull, Acta Metall. 1969; 17: 1021.*

# Bulk formation of a metallic glass: $Pd_{40}Ni_{40}P_{20}$

- Suppression of homogeneous nucleation:
  Alloy Selection: Consideration of $T_{rg}$

  * $Pd_{82}Si_{18}$ ➡ $T_{rg}$=0.6
  - Homogeneous nucleation rate: $>10^5/cm^3s$
  - Critical cooling rate: > 800 K/s

  * $Pd_{77.5}Cu_6Si_{16.5}$ ➡ $T_{rg}$=0.64

  * $Pd_{40}Ni_{40}P_{20}$ ➡ $T_{rg}$=0.67
  $T_g$=590 K, $T_e$ = 880 K, $T_l$ = 985 K

<Schematic diagram of apparatus>

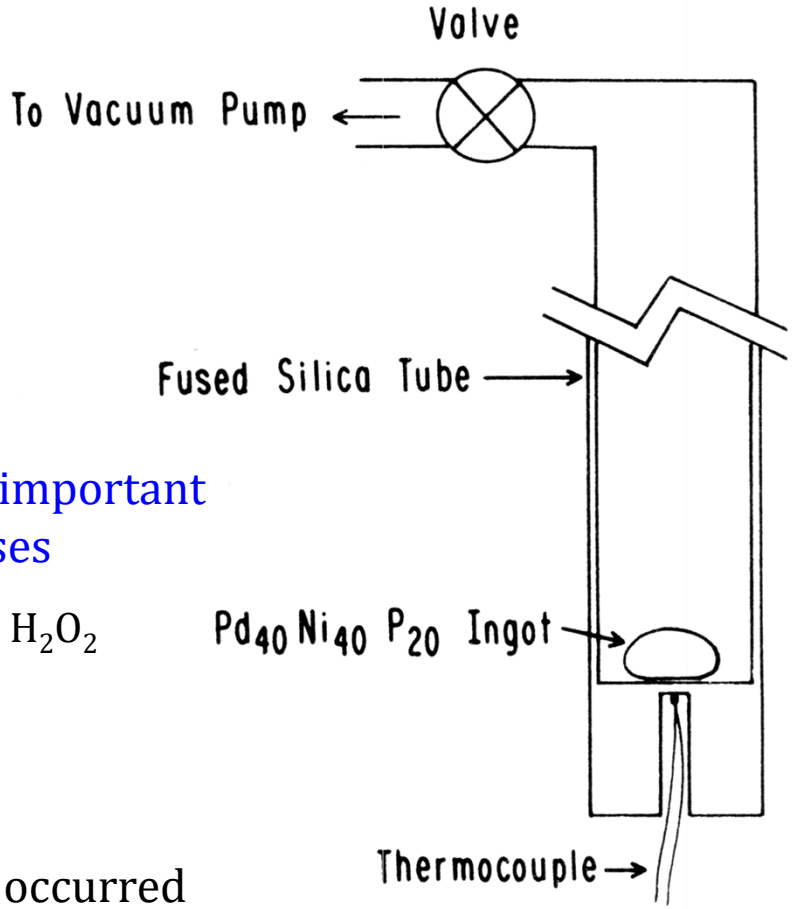


- Suppression of Heterogeneous nucleation: very important in suppressing the nucleation of crystalline phases

  1. Surface Etching of ingot in a mixture of HCL and $H_2O_2$
     : elimination of surface heterogeneities

  2. Thermal cycling –5 cycles
     : dissolution of nucleating heterogeneities
  → reduce the temperature at which nucleation occurred

# Bulk formation of a metallic glass: $Pd_{40}Ni_{40}P_{20}$

Heat and cool the molten metal

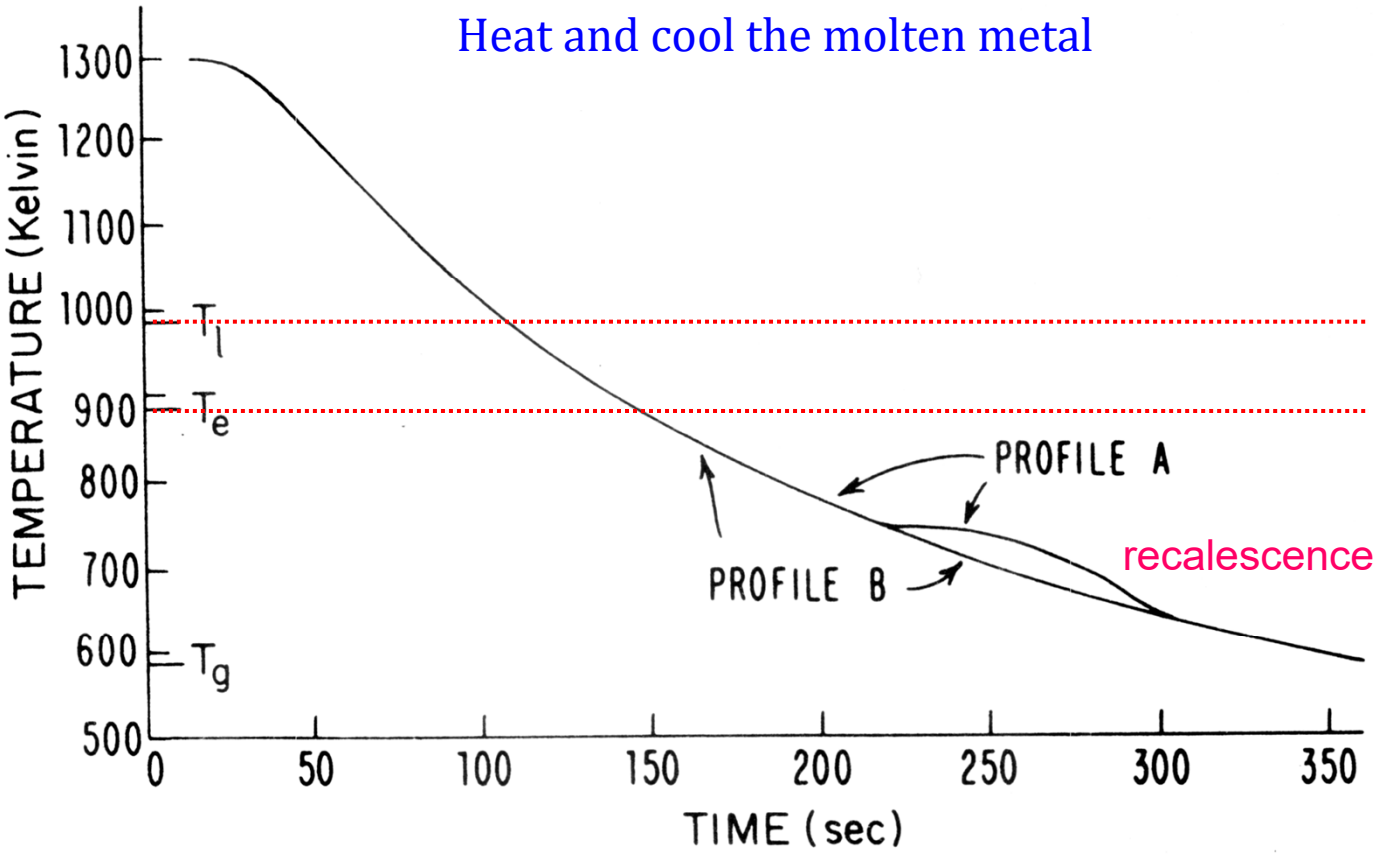


FIG. 2. Superposition of two cooling profiles: A—bulk crystallization which began at 740 K. B—formation of a glassy ingot.

*A.J. Drehman, A.L. Greer, D. Turnbull, Appl. Phys. Lett. 1982; 41: 716.*

# Bulk formation of a metallic glass: $Pd_{40}Ni_{40}P_{20}$

- Largest ingot

- minimum dimension 0.6 cm and mass of 2.3 g

- Critical cooling rate: ~ 1.4 K/sec.

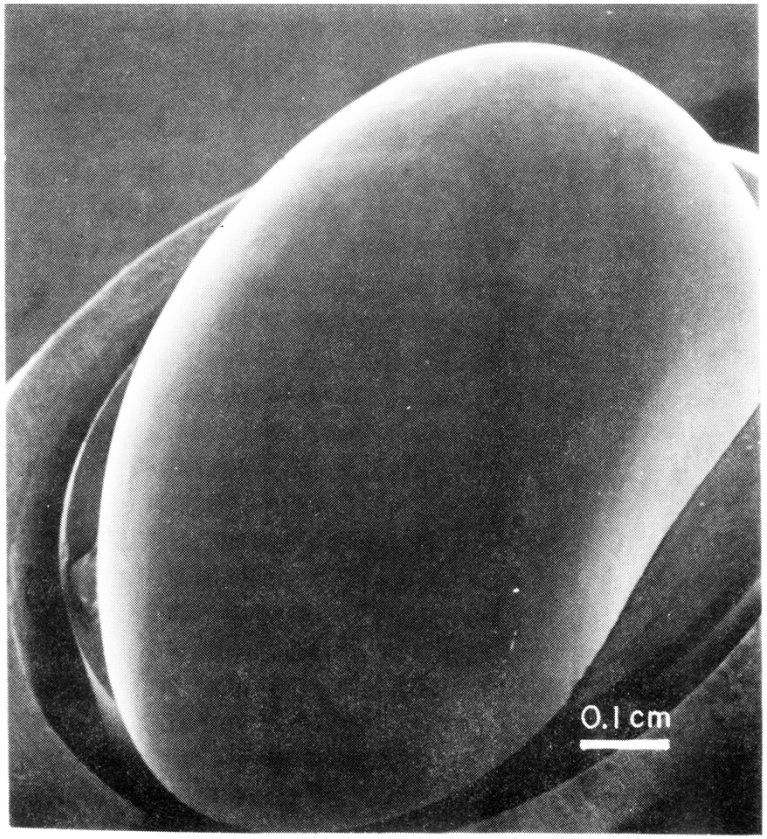


*Appl. Phys. Lett. 1982; 41: 716.

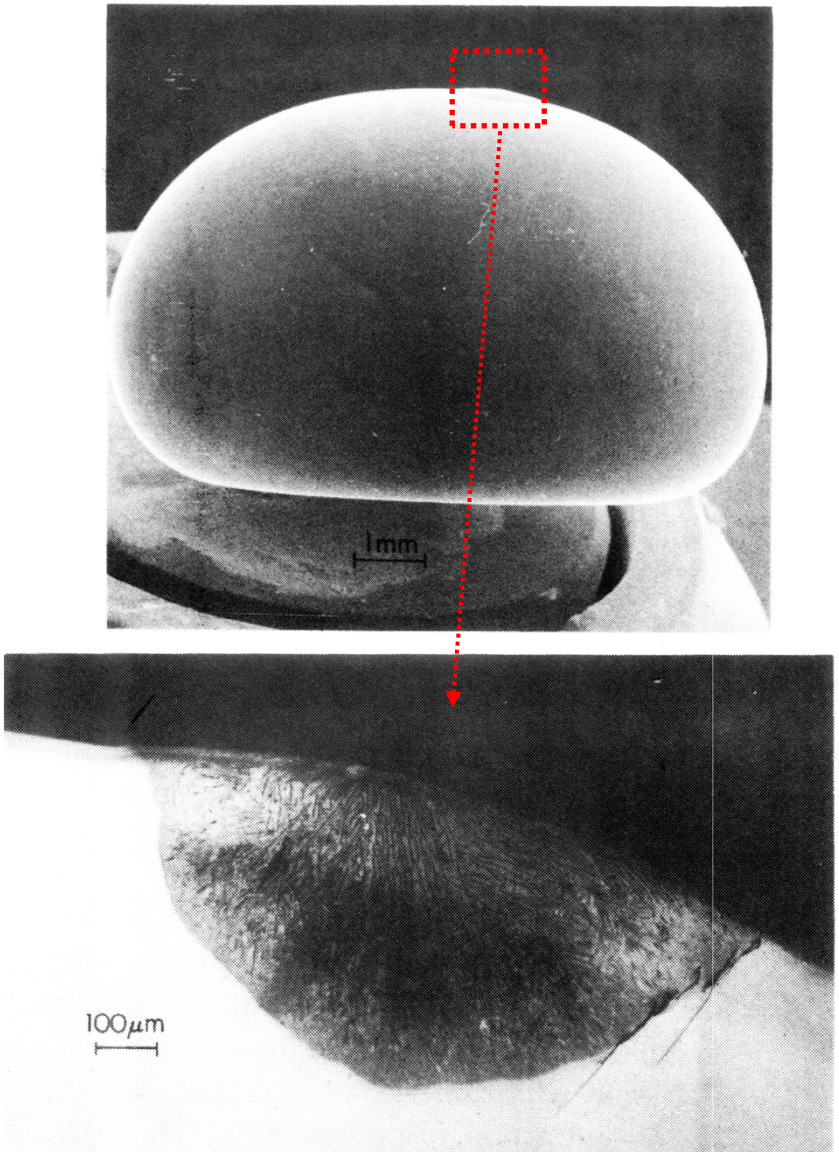


OM image of the cross section of a crystalline inclusion showing the eutectic structure

4.5.1 Flux Melting Technique : immersed in molten oxide flux

# Formation of bulk metallic glass by fluxing

- Heterogeneous nucleation

1. Surface oxide layer
2. Container walls
3. Motes in the liquid

➡ Suppression

1. Ingot = Chemical etching
   by dilute aqua regia ($HNO_3$ + HCl)
2. Interior of the vessel = Cleaning
   by hydrofluoric acid
3. Impurities = Successive heating-cooling cycles
   in a molten oxide flux

$B_2O_3$ melting point 723 K, boiling point <40,000 K

After gravity segregation to the oxide-metal interface most heterophase impurities presumably are dissolved or deactivated (e.g., by being wet) by the molten oxide (like slag in foundries)

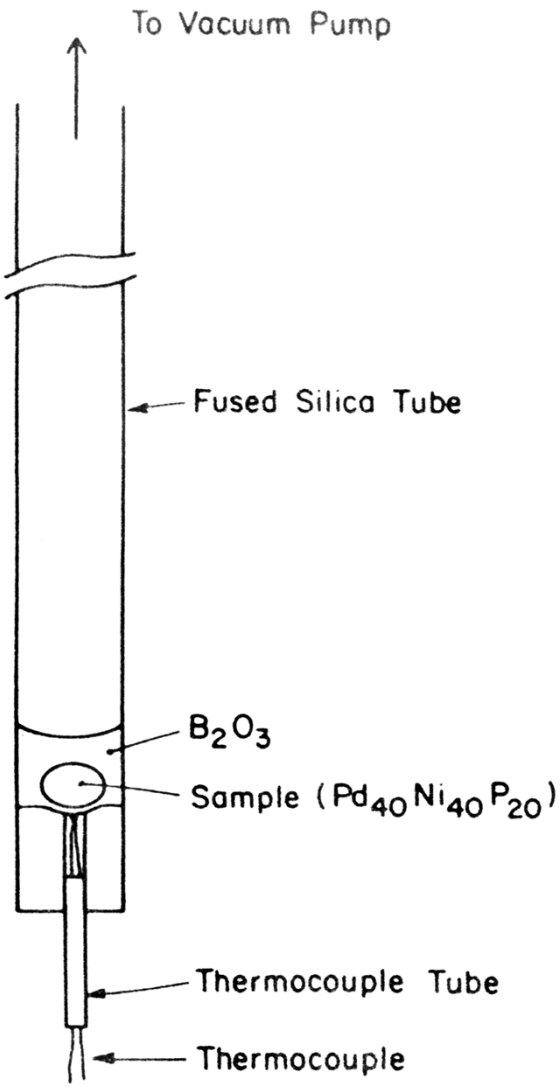

# Schematic process of fluxing

: 1273K →cooling→ $B_2O_3$ still in the molten state at $T_g$ of $Pd_{40}Ni_{40}P_{20}$ (600K) ?

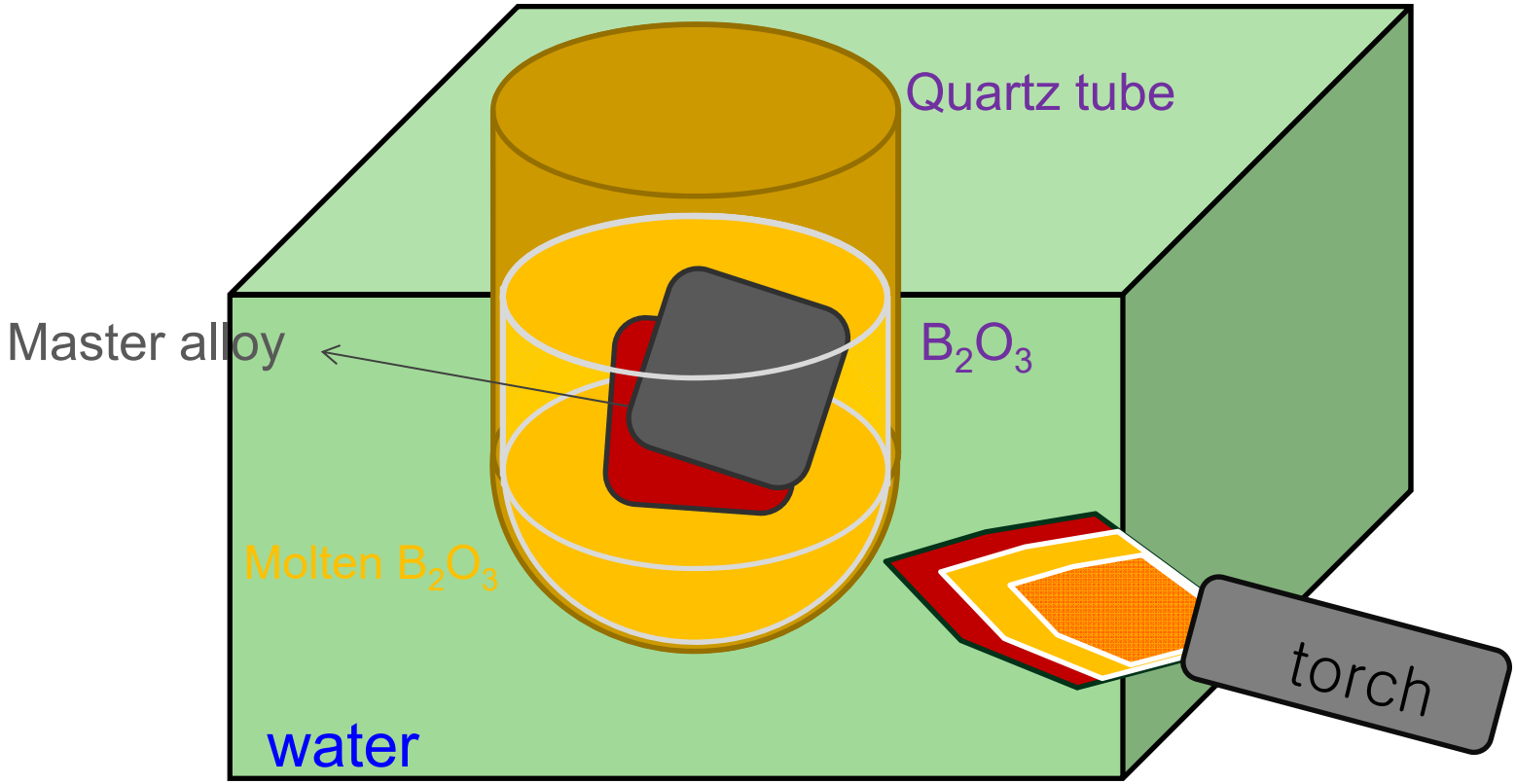


**$B_2O_3$ smelting point 723K (trigonal), Boiling point 2133 K**

# Formation of centimeter-sized BMG by fluxing

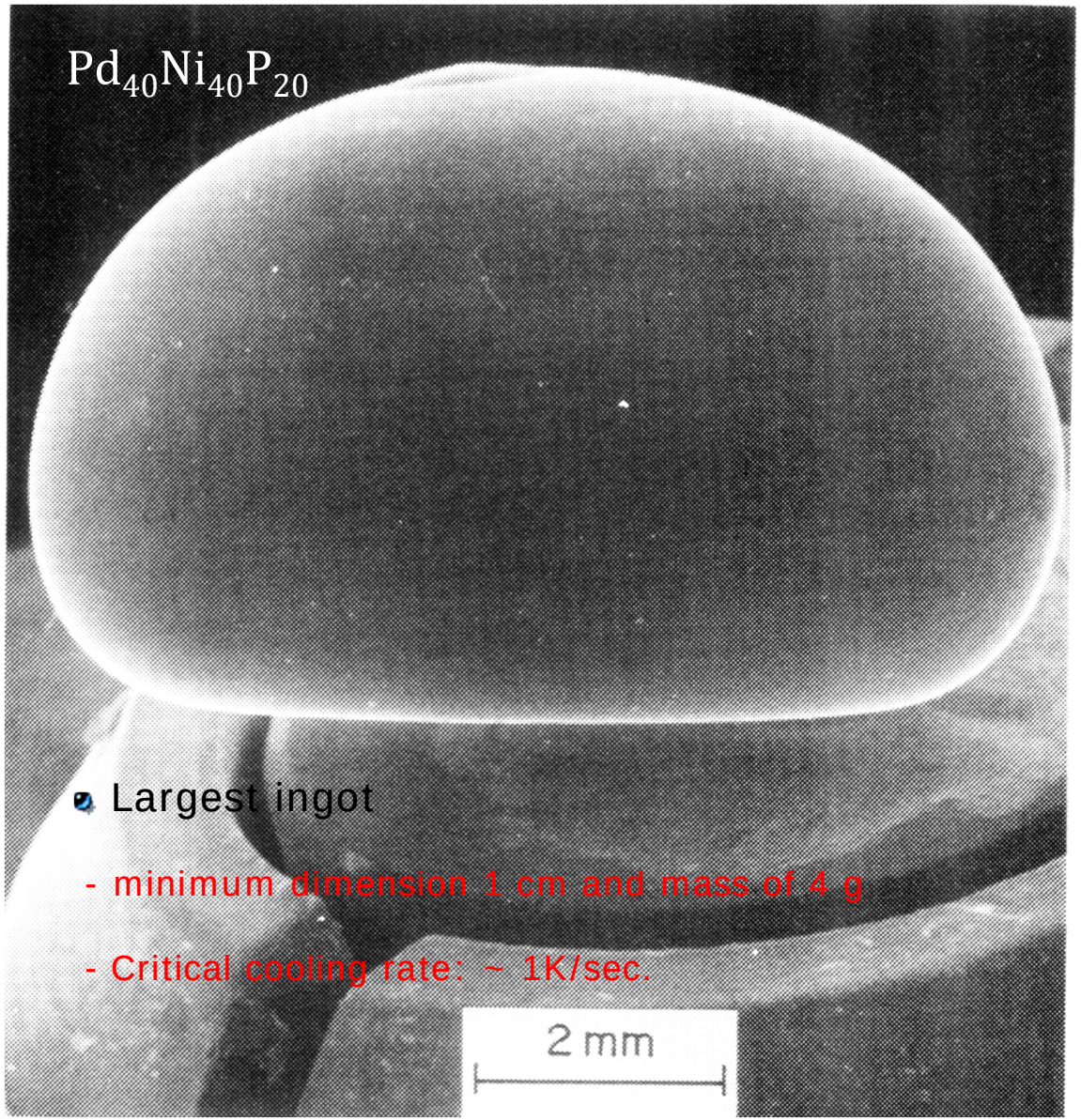

# Formation of centimeter-sized BMG by fluxing

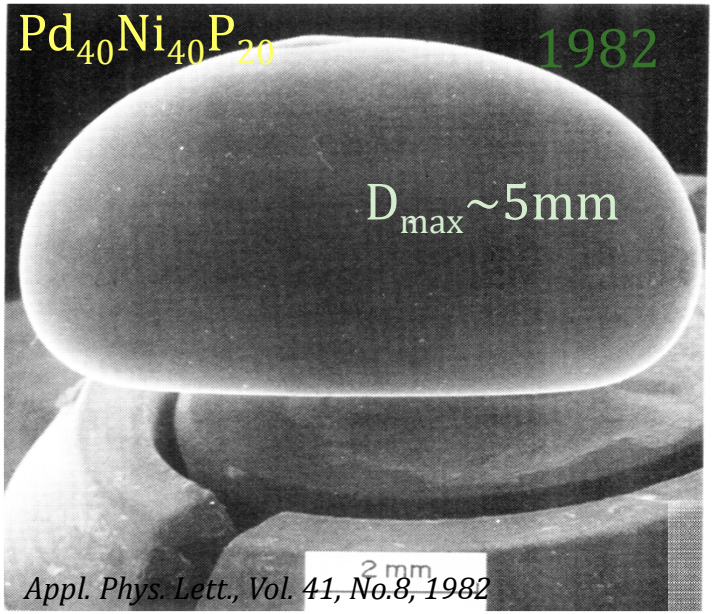


1984

$D_{max}$~10mm

After fluxing treatment

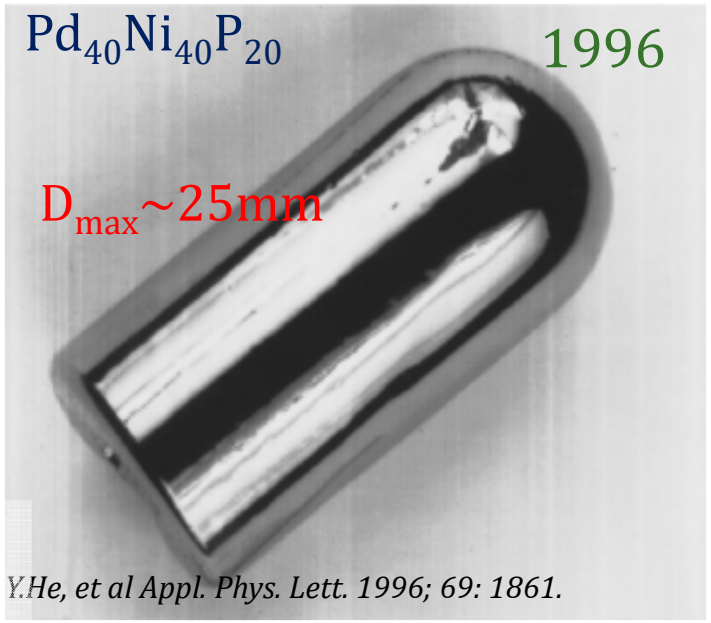


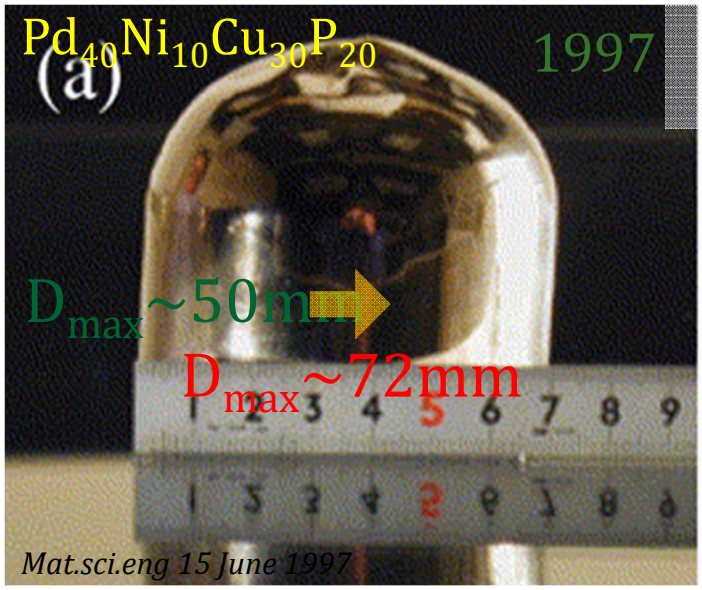


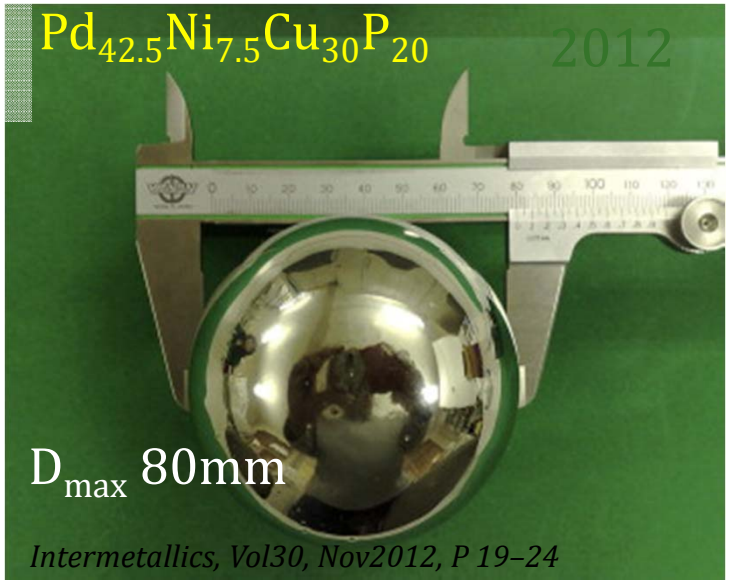

**TABLE 4.1**

Summary of Early Results on Discovery of BMGs

| Alloy Composition | Critical Cooling Rate (K $s^{-1}$) | Year of Discovery | Largest Section Thickness (mm) | Reference |
|---|---|---|---|---|
| $(Pd_{1-x}M_x)_{0.835}Si_{0.165}$ (M = Cu, Ag, Au, Fe, Co, Ni) | — | 1974 | 1–3 | [18] |
| $(Pd_{1-x}T_x)_{1-xP}P_{xP}$ or $(Pt_{1-x}T_x)_{1-xP}P_{xP}$ (T = Fe, Co, or Ni) | — | 1974 | 1–3 | [18] |
| $Pd_{40}Ni_{40}P_{20}$ | 1 | 1982 | 5 | [20] |
| $Pd_{40}Ni_{40}P_{20}$ (flux treated) | — | 1984 | 10 | [21] |
| $La_{55}Al_{25}Ni_{20}$ | — | 1989 | 1.2 | [23] |
| $Mg_{65}Cu_{25}Y_{10}$ | — | 1992 | 7 | [24] |
| $Zr_{41.2}Ti_{13.8}Cu_{12.5}Ni_{10}Be_{22.5}$ | ~1 | 1993 | 14 | [25] |
| $Pd_{40}Ni_{10}Cu_{30}P_{20}$ | 1.57 | 1996 | 40 | [26] |
| $Pd_{40}Ni_{10}Cu_{30}P_{20}$ (flux treated) | 0.1 | 1997 | 72 | [19] |

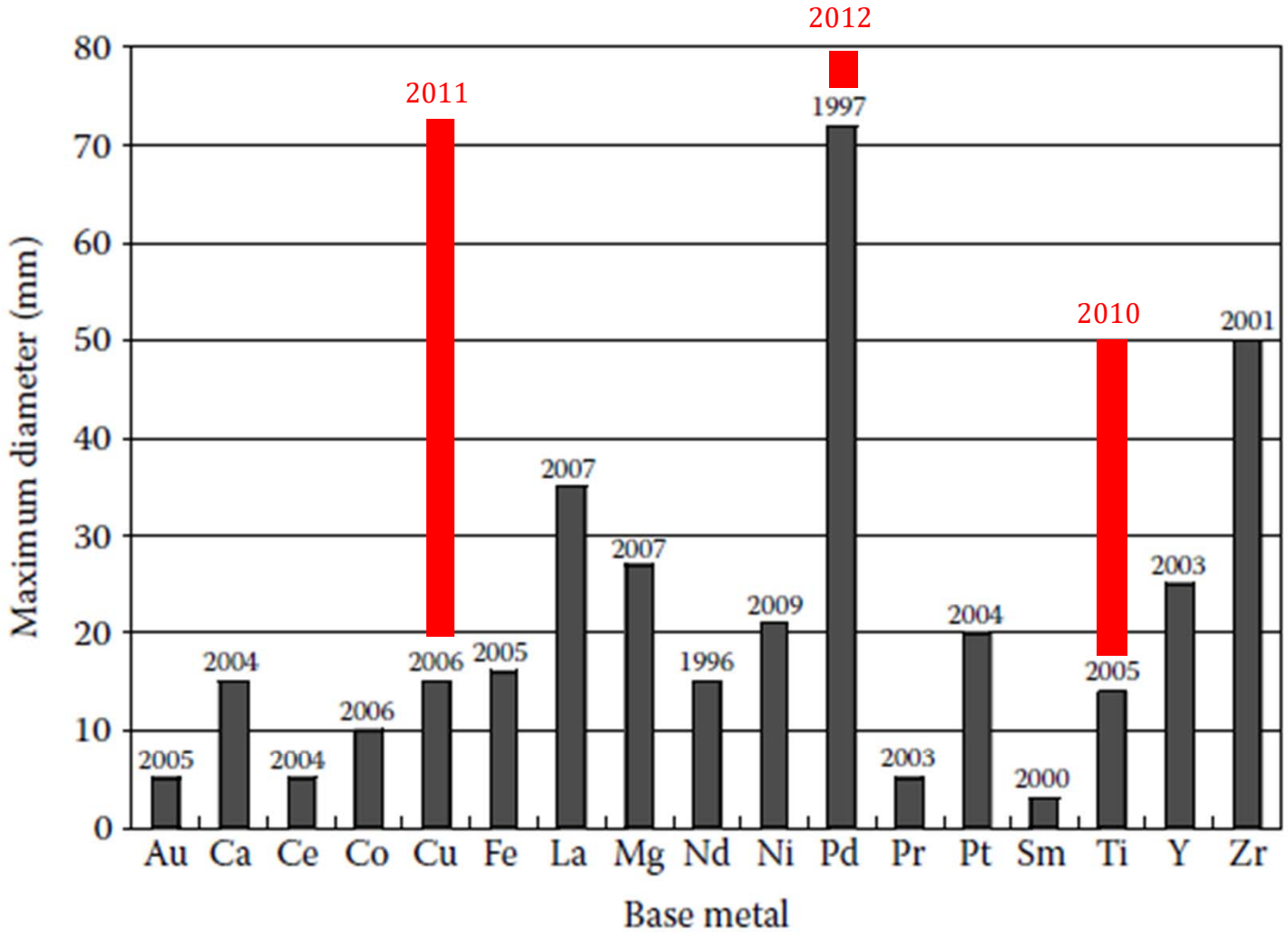


**FIGURE 2.7**
Maximum diameters of the BMG rods achieved in different alloy systems and the years in which they were discovered.

# Bulk glass formation in the Pd-/Ni-/Cu-/Zr- element system

**Massy Ingot Shape**

(a) Pd-Cu-Ni-P

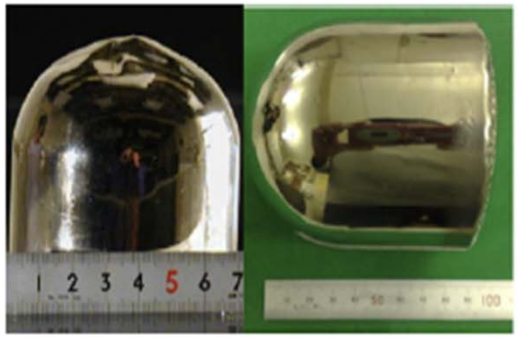

72ϕx 75 mm 80ϕx 85 mm

(b) Zr-Al-Ni-Cu

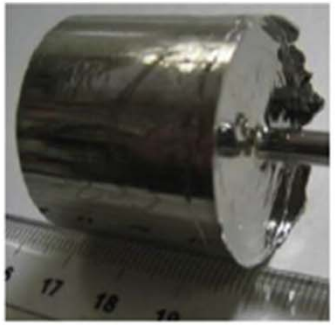

(c) Cu-Zr-Al-Ag

(d) Ni-Pd-P-B

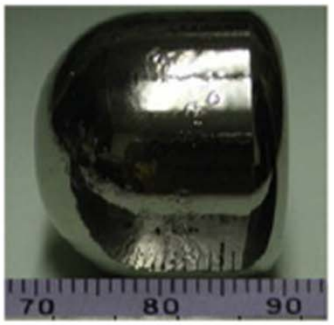

**Cylindrical Rods**

(e) Pd-Cu-Ni-P

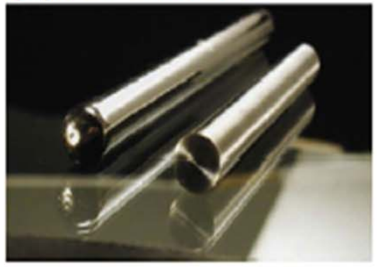

(f) Pt-Pd-Cu-P

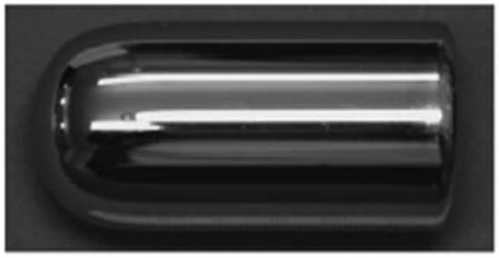

**Hollow Pipes**

(g) Pd-Cu-Ni-P

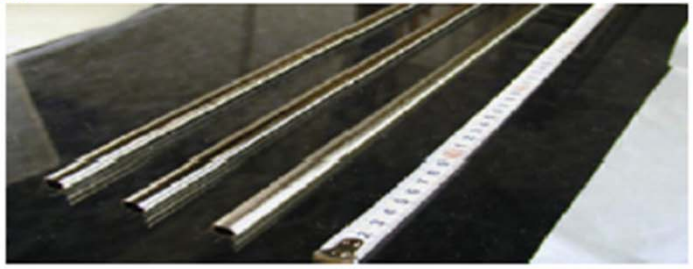

## 4.5.2 Role of Contamination

Zirconium and Titanium based BMG: very sensitive to the presence of impurities

Ex) - high oxygen contents reduced the supercooled liquid region and changed the crystallization behavior (formation of quasicrystals) in Zr based BMGs.

- it is possible that other interstitial elements may also have a significant effect like O.

1) Crystallization incubation tied decreased by orders of magnitude as one went from 250 to 5250 ppm of oxygen (oxygen content↑→ incubation time ↓)

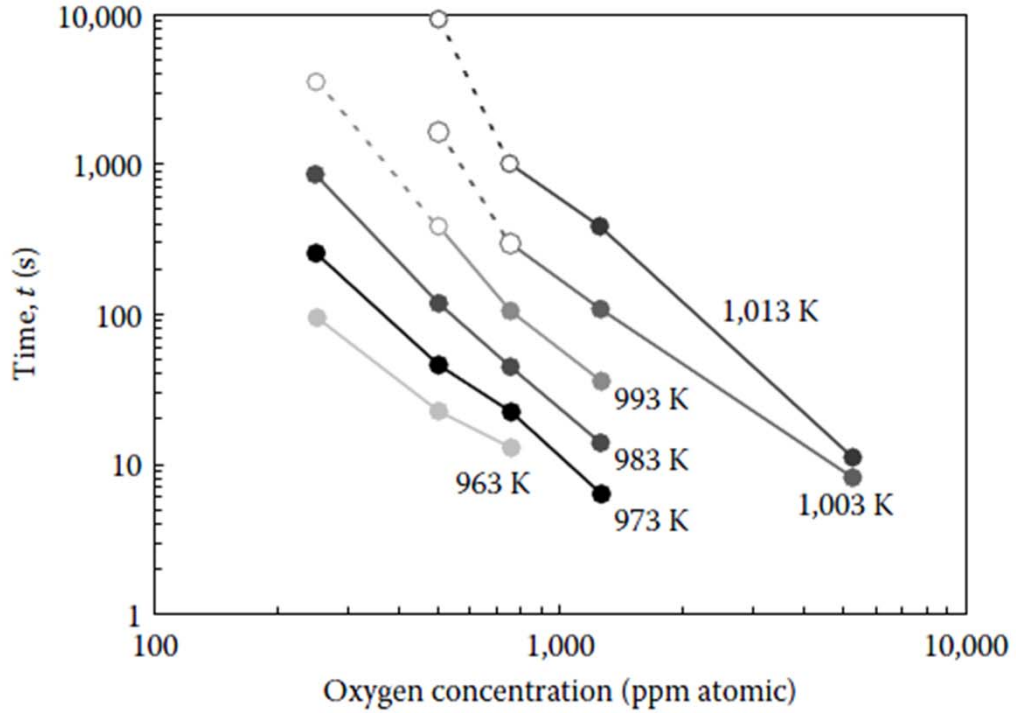


**FIGURE 4.2**
Crystallization incubation time at different temperatures as a function of oxygen content in a $Zr_{52.5}Ti_5Cu_{17.9}Ni_{14.6}Al_{10}$ bulk glassy alloy. (Reprinted from Lin, X.H. et al., *Mater. Trans., JIM*, 38, 473, 1997. With permission.)

# Effect of Oxygen Impurity on Crystallization of an Undercooled Bulk Glass Forming Zr–Ti–Cu–Ni–Al Alloy

X. H. Lin*, W. L. Johnson* and W. K. Rhim**

*W. M. Keck Laboratory of Engineering Materials, California Institute of Technology, Pasadena, CA 91125, USA

**Jet Propulsion Laboratory, California Institute of Technology, Pasadena, CA 91109, USA

High vacuum, containerless, electrostatic levitation process has been used to study the undercooling and crystallization kinetics of a bulk glass forming Zr–Ti–Cu–Ni–Al alloy. The oxygen impurity level in the alloy has been found to play a crucial role in the crystallization kinetics of the undercooled melt.

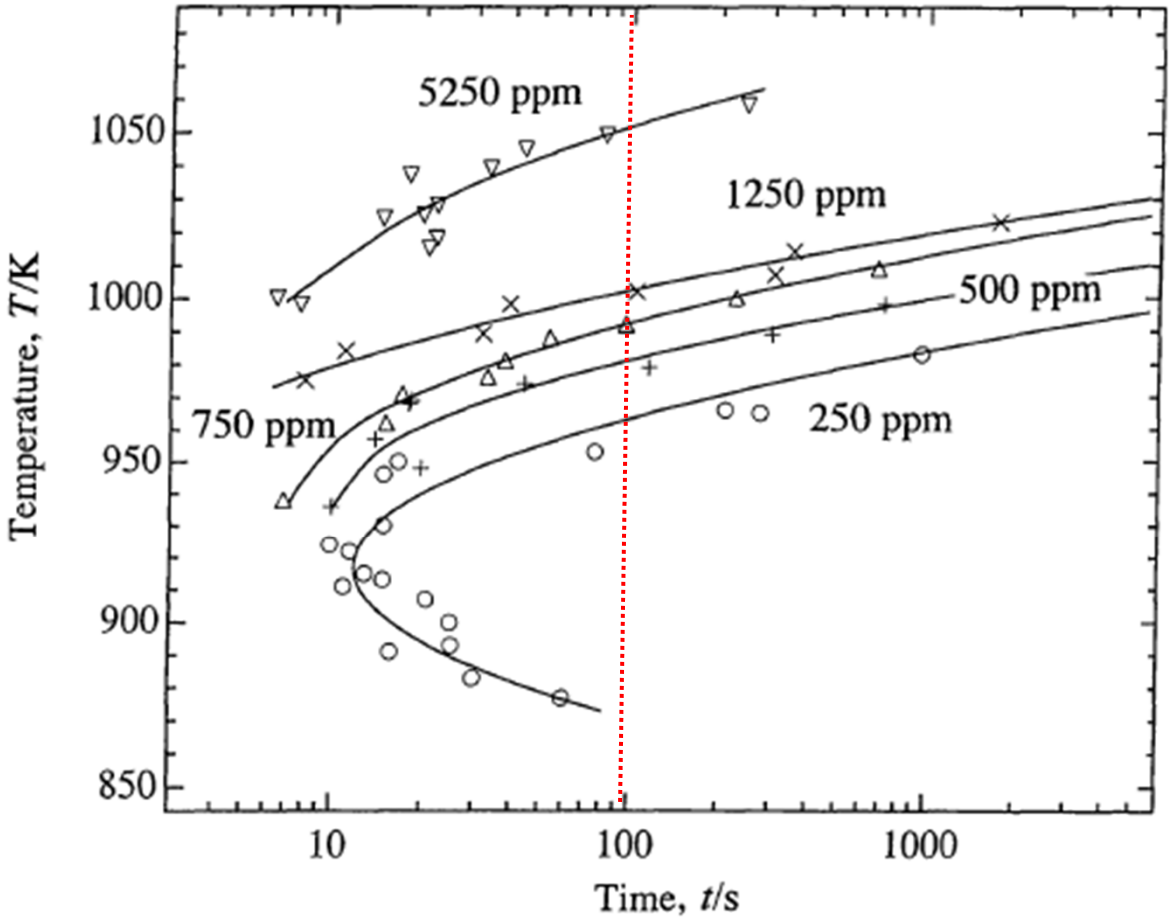


Fig. 5 Time-temperature-transformation diagrams of alloys of 5250, 1250, 750, 500 and 250 atom ppm oxygen respectively.

2) Effect of oxygen content (0.28-0.6 at.%) on the thermal stability of the glassy phase

: GFA decreased with increasing oxygen content. (oxygen content↑→$T_g$↑ & $T_x$↓)

→ need to careful in directly correlating the extent of SLR with the high GFA of alloys especially in reactive alloy system such as those based on Zirconium or Titanium

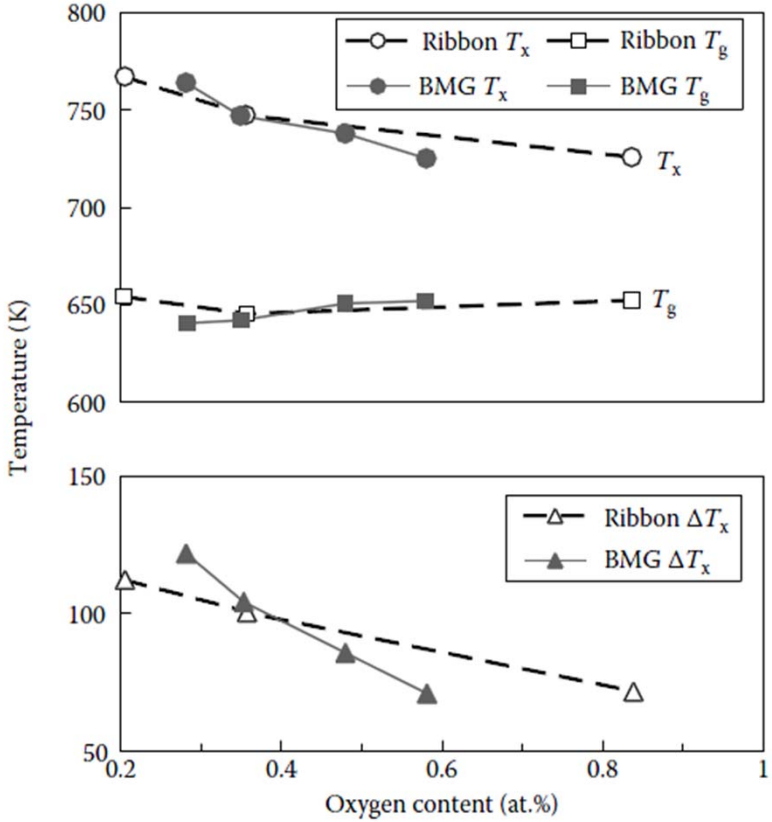


**FIGURE 4.3**
Variation of $T_g$, $T_x$, and $\Delta T_x$ as a function of the oxygen content in the Zr-glassy alloys. Results for both bulk samples and melt-spun ribbons are shown. (Reprinted from Gebert, A. et al., *Acta Mater.*, 46, 5475, 1998. With permission.)

➡ **Scavenger effect**: addition of strong oxide-forming elements →reduce oxygen content → GFA↑

ex) $Zr_{52.5}Cu_{17.9}Ni_{14.6}Al_{10}Ti_5$ with 0.03-0.06 at.%Sc → $Sc_2O_3$↑→ GFA↑ up to 12mm

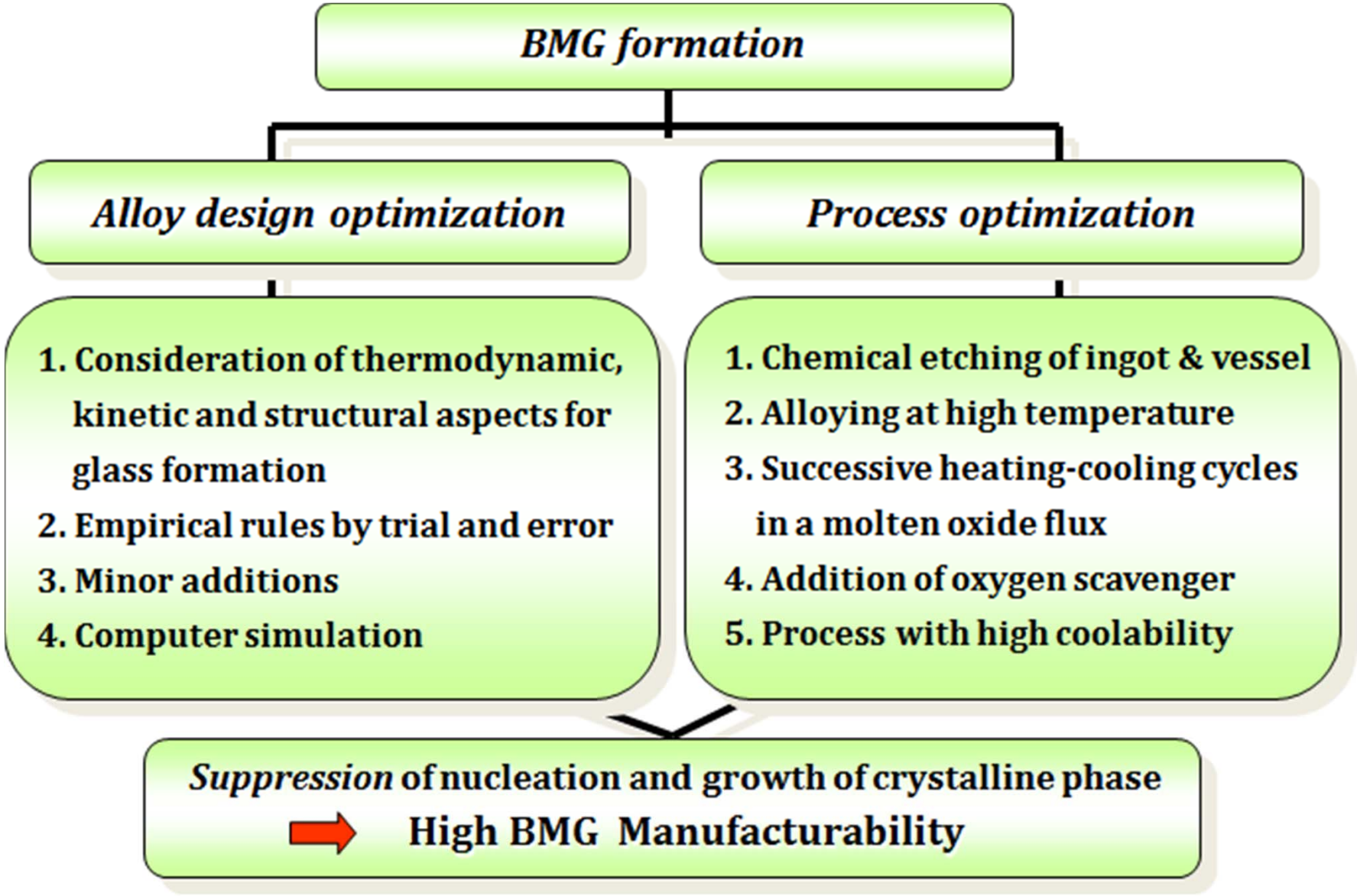
BMG formation
Alloy design optimization
Process optimization
1. Consideration of thermodynamic, kinetic and structural aspects for glass formation
2. Empirical rules by trial and error
3. Minor additions
4. Computer simulation
1. Chemical etching of ingot & vessel
2. Alloying at high temperature
3. Successive heating-cooling cycles in a molten oxide flux
4. Addition of oxygen scavenger
5. Process with high coolability
Suppression of nucleation and growth of crystalline phase
High BMG Manufacturability

## 4.6 Bulk Metallic Glass Casting Methods

**4.6.1 Water-Quenching Method** : simplest of the quenching methods used for centuries to harden steel (by transforming the soft austenite to the hard martensite phase)

- Cooling rate: about 10-100 K/s, inherently dependent on the heat transfer efficiency of quenching medium, the size of the specimen, and its heat transfer properties.

- A distinct advantage of the water-quenching method is that due to the slow solidification rates, the cast specimen contains much less residual stresses and porosity.

### The world's biggest glassy alloy ever made

Intermetallics 30 (2012) 19–24

Nobuyuki Nishiyama [a,*], Kana Takenaka [a], Haruko Miura [a], Noriko Saidoh [a], Yuqiao Zeng [b], Akihisa Inoue [b]

[a] RIMCOF Tohoku Univ. Lab., The Materials Process Technology Center, Sendai 980-8577, Japan
[b] Institute for Materials Research, Tohoku University, Sendai 980-8577, Japan

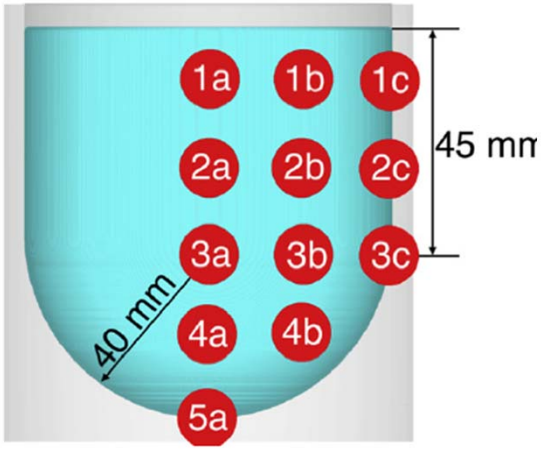


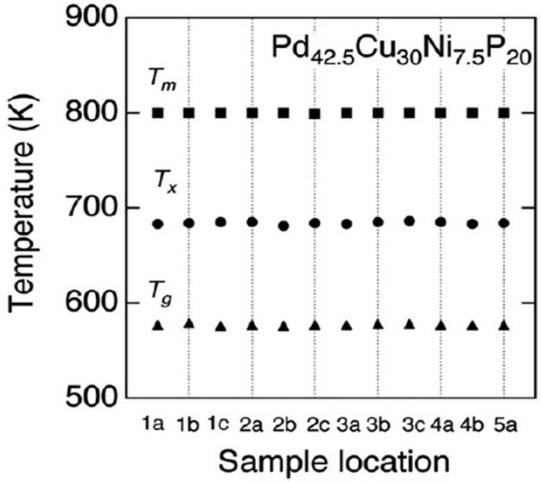


**TABLE 4.2**

Details of Bulk Metallic Glassy Rods Produced by the Water Quenching Method

| Alloy System | Diameter of the Rod (mm) | Critical Cooling Rate (K $s^{-1}$) | Year | Reference |
|---|---|---|---|---|
| $(Pd_{1-x}M_x)_{0.835}Si_{0.165}$ | 1–3 | $<10^3$ | 1974 | [18] |
| $(Pd_{1-x}T_x)_{1-xP}P_{xP}$ | 1–3 | $<10^3$ | 1974 | [18] |
| $(Pt_{1-x}Ni_x)_{1-xP}P_{xP}$ | 1–3 | $<10^3$ | 1974 | [18] |
| $Pd_{40}Ni_{40}P_{20}$ | 5–6 | ~1 | 1982 | [20] |
| $Pd_{40}Ni_{40}P_{20}$ (flux treated) | 10 | | 1984 | [21] |
| $Zr_{65}Al_{7.5}Ni_{10}Cu_{17.5}$ | <16 | 1.5 | 1993 | [37] |
| $Zr_{41.2}Ti_{13.8}Cu_{12.5}Ni_{10}Be_{22.5}$ | 14 | <10 | 1993 | [25] |
| $Pd_{40}Cu_{30}Ni_{10}P_{20}$ | 40 | 1.57 | 1996 | [26] |
| $Pd_{40}Cu_{30}Ni_{10}P_{20}$ (flux treated) | 50–72 | 0.1 | 1997 | [19] |
| $Pd_{40}Ni_{40}P_{20}$ | 7 | 100 | 1999 | [38] |
| $Pd_{40}Ni_{32.5}Fe_{7.5}P_{20}$ | 7 | 100 | 1999 | [38] |
| $Pd_{40}Ni_{20}Fe_{20}P_{20}$ | 7 | 100 | 1999 | [38] |
| $Mg_{65}Y_{10}Cu_{15}Ag_5Pd_5$ | 12 | | 2001 | [39] |
| $Y_{56}Al_{24}Co_{20}$ | 1.5 | | 2003 | [40] |
| $Y_{36}Sc_{20}Al_{24}Co_{20}$ | 25 | | 2003 | [40] |
| $Pt_{60}Cu_{20}P_{20}$ | <4 | | 2004 | [41] |
| $Pt_{60}Cu_{16}Co_2P_{22}$ (flux treated) | 16 | | 2004 | [41] |
| $Pt_{57.5}Cu_{14.7}Ni_{5.3}P_{22.5}$ (flux treated) | 16 | | 2004 | [41] |
| $Pt_{42.5}Cu_{27}Ni_{9.5}P_{21}$ (flux treated) | 20 | | 2004 | [41] |

Most common container material: Quartz but compatibility between melt and the crucible _important issue

For MG BMG, when a quartz tube was used, Si dissolved in the Mg melt as an impurity and acted as heterogeneous nucleation sites. Consequently, the GFA of the alloy was reduced. On the other hand, when an iron tube was used, there was no interaction between iron and the Mg-melt. → $D_{max}$ = 12 mm

## 4.6 Bulk Metallic Glass Casting Methods

### 4.6.2 High-Pressure Die Casting

: offer high solidification rates (because heat is extracted more rapidly by the metal mold due to good contact), high productivity, low casting defect,
and possible to produce more complex shapes even in alloys with a high viscosity

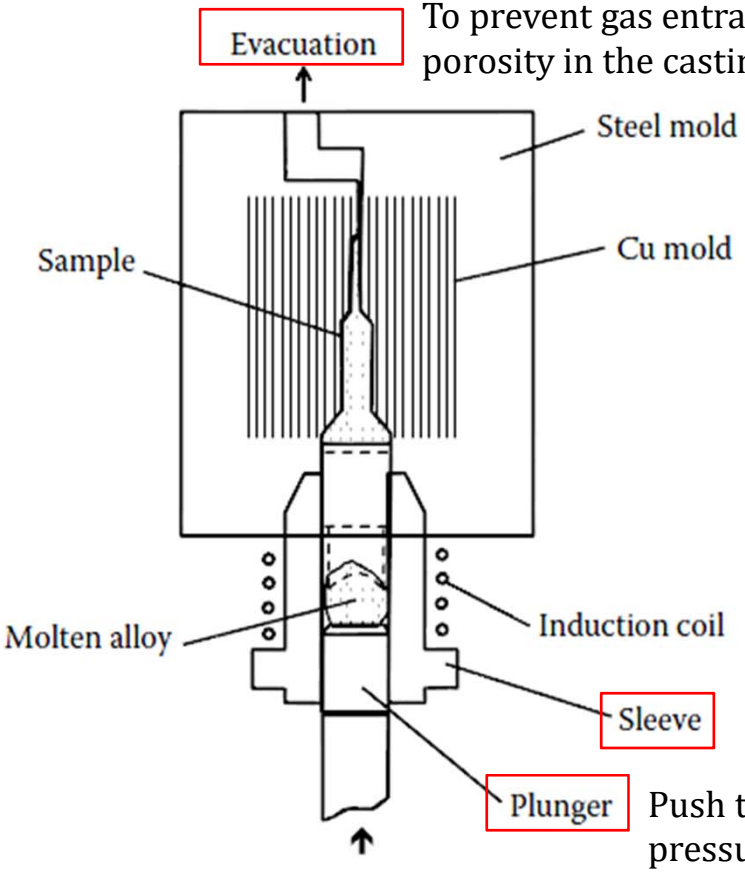


To prevent gas entrapment by the melt and consequent porosity in the casting

Melt the alloy

Push the molten alloy through hydraulic pressure into the Cu mold
Ex) 63 MPa, 1.7m/s, hold time of 5s

**FIGURE 4.5**
Schematic diagram of the high-pressure die casting equipment designed and used by Inoue et al. (Reprinted from Inoue, A. et al., *Mater. Trans., JIM*, 33, 937, 1992. With permission.)

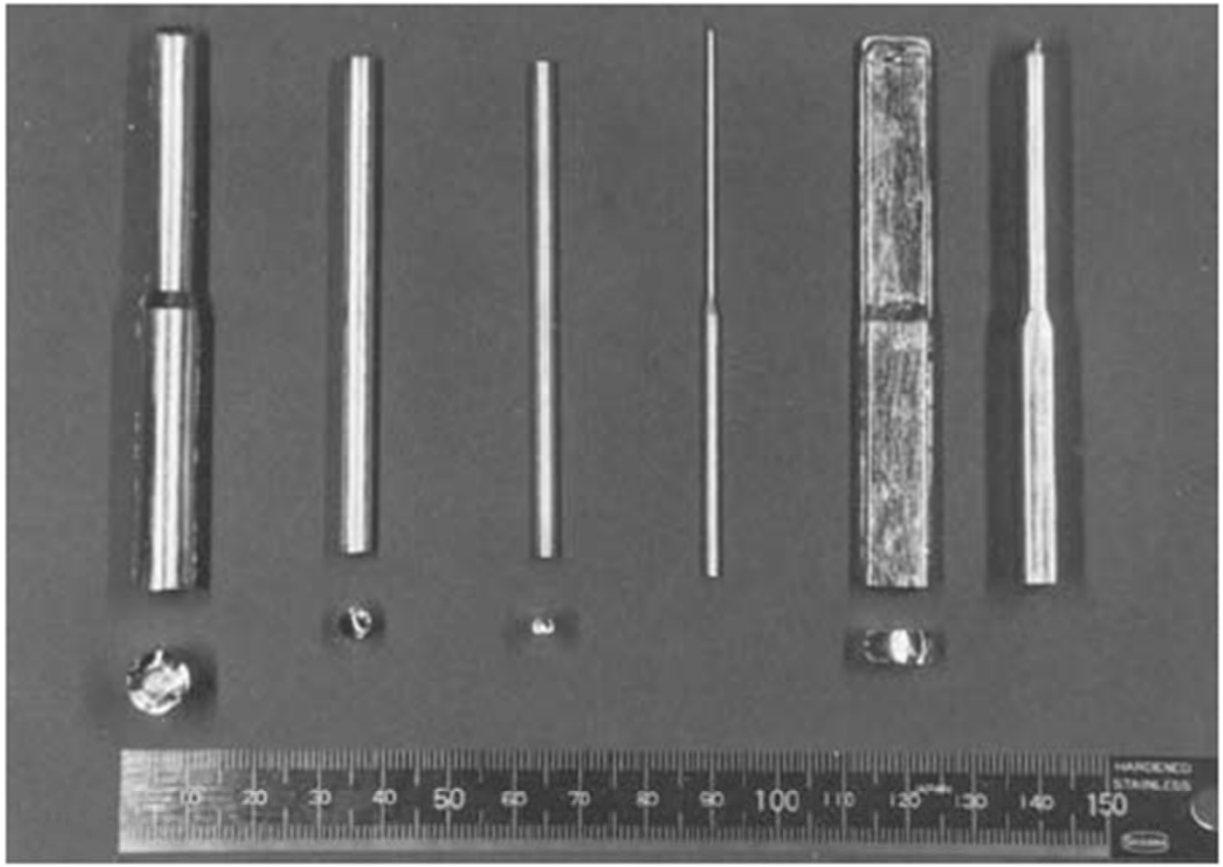


**FIGURE 4.6**
Photographs of the $Mg_{65}Cu_{25}Y_{10}$ rods and sheets (of different diameters) produced by the high-pressure die-casting technique. The length of the samples is 80 mm and the thickness or diameter varies from 0.5 to 9 mm. Note the bright and shiny appearance of both the types of samples. (Reprinted from Inoue, A. et al., *Mater. Trans., JIM*, 33, 937, 1992. With permission.)

# 4.6 Bulk Metallic Glass Casting Methods

## 4.6.6 Squeeze-casting Method

: involves solidification of the molten metal under a high pressure within a closed die by utilizing a hydraulic pressure → Net-shape forming capability, fully dense sample

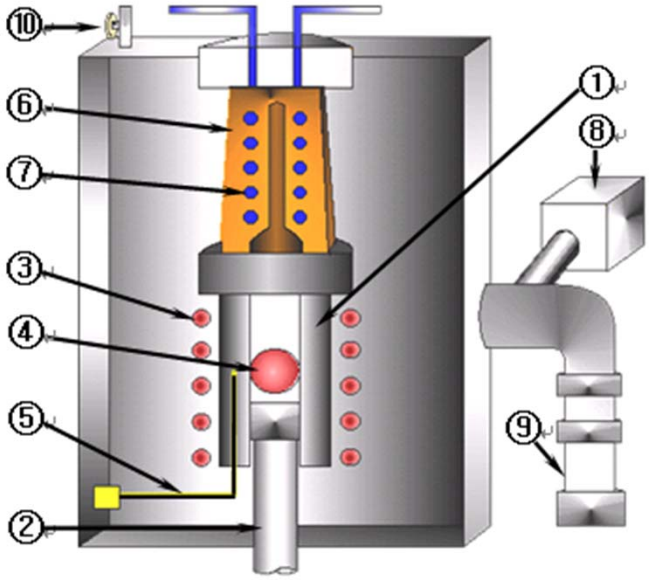


| | | | |
|---|---|---|---|
| ① | Graphite crucible | ⑥ | Copper mold |
| ② | Plunger | ⑦ | Water cooling |
| ③ | Induction coil | ⑧ | Rotary pump |
| ④ | Molten alloy | ⑨ | Diffusion pump |
| ⑤ | Thermocouple | ⑩ | Evacuation valve |

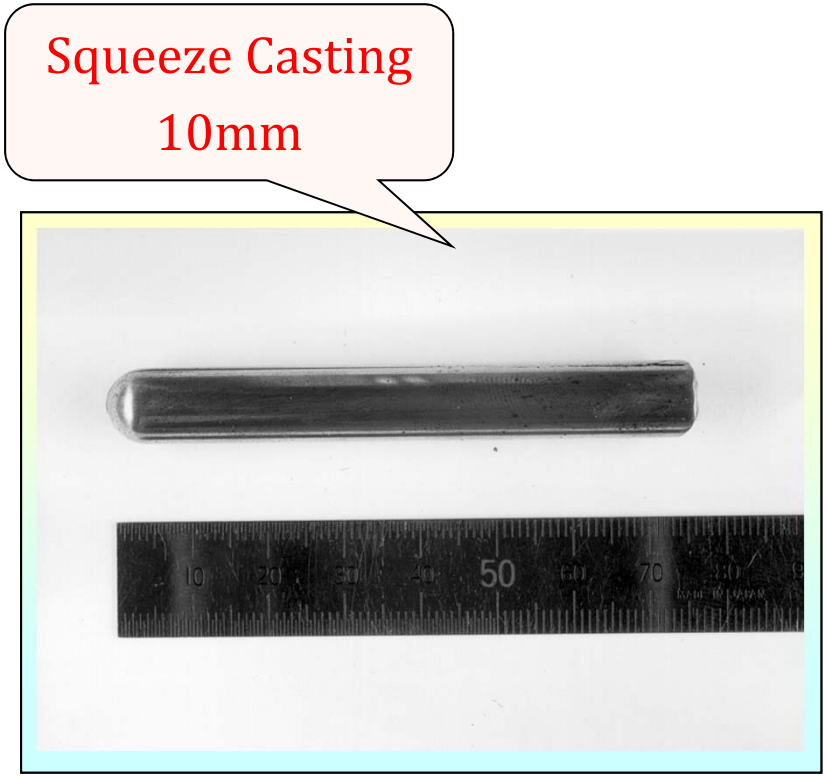


Push the molten alloy through hydraulic pressure into the Cu mold

Ex) 100 MPa, hold time of 2min until the liquid alloy completely solidified

→ Undercooling to much below the equilibrium solidification temperature

# Gibbs Free Energy as a Function of Temp. or Pressure

Considering P, T $G = G(T, P)$

$$dG = VdP - SdT$$

$$G(P,T) = G(P_0,T_0) + \int_{P0}^{P1} V(T_0,P)dP - \int_{T0}^{T1} S(P,T)dT$$

## 1) Temperature Effects

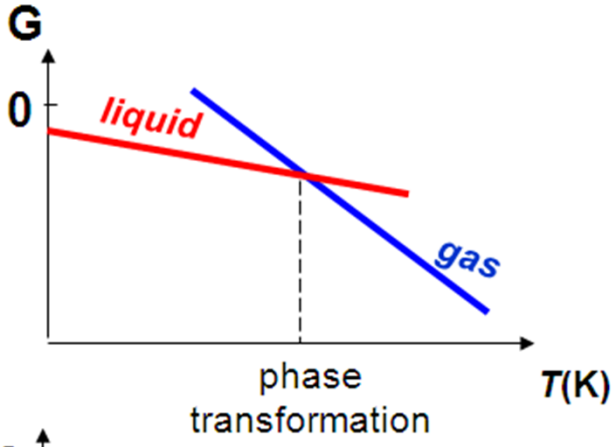


**S**(water) = 70 J/K

**S**(vapor) = 189 J/K

$$\left(\frac{\partial G}{\partial T}\right)_P = -S$$

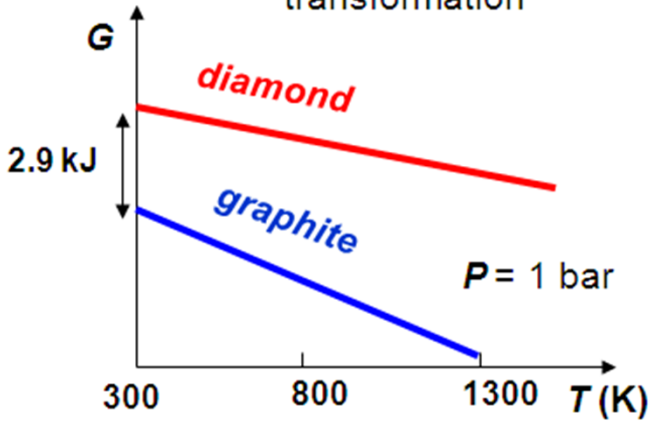


**S**(graphite) = 5.74 J/K,
**S**(diamond) = 2.38 J/K,

## 2) Pressure Effects

**If the two phases in equilibrium have different molar volumes, the only way to maintain equilibrium at different pressures is by varying the equilibrium temperature.**

If α, β phases are equilibrium,

$$dG^{\alpha} = V^{\alpha}dP - S^{\alpha}dT$$

$$dG^{\beta} = V^{\beta}dP - S^{\beta}dT$$

At equilibrium,

$$dG^{\alpha} = dG^{\beta}$$

$$\left(\frac{dP}{dT}\right)_{eq} = \frac{S^{\beta} - S^{\alpha}}{V^{\beta} - V^{\alpha}} = \frac{\Delta S}{\Delta V}$$

where, $\Delta S = \frac{\Delta H}{T_{eq}}$

$$\left(\frac{dP}{dT}\right)_{eq} = \frac{\Delta H}{T_{eq}\Delta V}$$

**: *Clausius-Clapeyron Relation***

**(applies to all coexistence curves)**

**On a pressure-temperature (P–T) diagram, the line separating the two phases is known as the coexistence curve. The Clausius–Clapeyron relation gives the slope of this curve.**

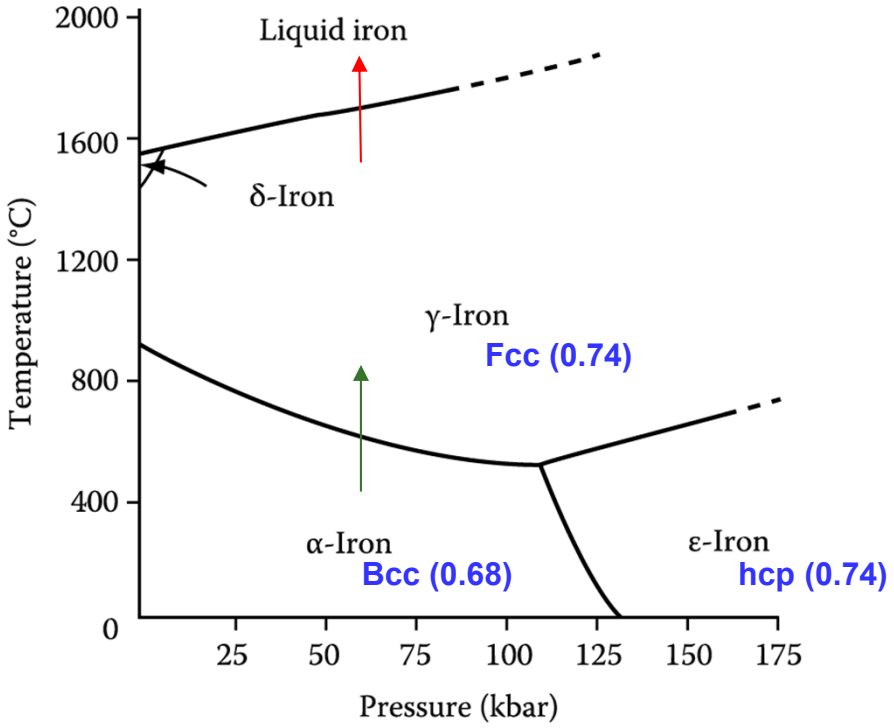


Fig. 1.5 Effect of pressure on the equilibrium phase diagram for pure iron

**Case 1. γ →liquid ; ΔV (+), ΔH(+)**

$$\left(\frac{dP}{dT}\right) = \frac{\Delta H}{T_{eq}\Delta V} > 0$$

**Case 2. α→γ ; ΔV (-), ΔH(+)**

$$\left(\frac{dP}{dT}\right) = \frac{\Delta H}{T_{eq}\Delta V} < 0$$

$$\left(\frac{\partial G}{\partial P}\right)_T = V$$

H6: Explain the role of P to improve GFA.